Department of Automatic Control and Systems Engineering

The University of Sheffield

PO Box 600, Mappin Street,

Sheffield S1 4DU,

UK

Interpretation and Utilisation of Parametric Models of Binary Distillation Columns: Relating Plant and Control Design

by

J. B. Edwards and S. B. Mohd Noor

(Process Control and Automation Research Group, AC&SE)

AC&SE Research Report No. 573 April 1995

Interpretation and Utilisation of Parametric Models of Binary Distillation Columns: Relating Plant and Control Design

J. B. Edwards and S. B. Mohd Noor

Abstract

Previously published analytical models [1], [2] for the separation dynamics of CSTC and tubular packed distillation columns are rederived using common notation for detailed comparison purposes. The separation and total composition equations are now successfully separated at an early stage in the derivation which is thus simplified. The analyses produce parametric formulae for steady-state separation and for the transfer-functions of both columns in terms of length, relative volatility, evaporation-and nominal vapour-rate parameters only plus column and end-vessel capacitance.

A second order, nonminimum-phase structure derived from high-and low-frequency asymptotic behaviour is shown to fit all types and, on the basis of this, analytic stability and critical error criteria for linear closed-loop control are derived: again requiring the substitution only of the above mentioned plant parameters. It is shown that, for equal parameters, tubular columns outperform CSTC types. However, matching of the two types for separation and stability is achievable by fictitious inflation of the CSTC length and volatility coefficient. This may permit use of an equivalent but simpler CSTC model for unified tubular plant and control design.

Finally the CSTC column is formulated as a parametric, bilinear third-order, state-space model having a state-dependent, input-coefficient matrix. This is derived with a view to future application of optimal control based on the on-line Riccatti solution method of Banks[3] already successfully tested on a bilinear CSTR chemical reactor model[4].

1. Introduction

Much research effort over the past 18 years within AC&SE at The University of Sheffield has been aimed at the derivation of parametric models of binary distillation columns of both the packed-and the tray-type. These have been derived from the basic physical equations of the process solved (in conjunction with the reboiler, feed and accumulator boundary conditions) by Laplace transform methods. Both spatially-distributed and lumped-parameter representations have been solved for large-signal steady-state behaviour and for the small signal response to sinusoidal inputs (i. e. for parametric transfer functions pertaining around the derived steady state operating point). Mol-fraction compositions of the top vapour and bottom liquid product have been the selected outputs whilst the perturbed inputs have been reboiler vapour and reflux liquid flowrates. Feed conditions have been kept fixed.

Since the main plant parameters and nominal quiescent input conditions appear explicitly in the derived response formulae (both large-signal, steady-state and TFM), these models have the potential (a) for uniting plant and control systems design and (b) for wide-ranging, fast-adaptive control. This report is the first of a series aimed at testing the extent to which there goals might be realised. The derivations of the presented parametric models have been published elsewhere by members of the Sheffield AC&SE Process Control Research Group past and present. The reader requiring such information should consult the references cited. This report is devoted to the response of composition separation between top and bottom products, (not to the average or total of these compositions. Previous research showed that, for a symmetrical column, deviations in separation and total are independently related to input perturbations in circulating flow rate and to differential product take-off rate respectively. With the benefit of this hindsight, the derivation of either relationship is capable of simplification by divorcing "separation" and "total" composition dynamics at a much earlier stage in the analysis. The resulting condensed versions for product separation are presented here therefore.

The report then proceeds to interpret the influence of plant parameters and operating conditions on large-signal steady state and small signal dynamic performance. Comparisons are made between columns modelled by (a) spatially distributed and by (b) lumped parameter representations: Using notation more familiar to Chemical Engineers, these will be referred to as (a) Tubular columns and (b) Continuous-stirred tank (columns): CSTC's. i.e.

(a) Tubular column means a column represented by a spatially distributed model

(b)CSTC means a column represented by a lumped parameter model

The terms long-and short columns have sometimes been used to distinguish the two types in the past but these are abandoned here since a long column may , in principle, be stirred whilst a CSTC process may be physically long. "Long" and "tubular" are therefore not necessarily synonymous. Nor are "short" and "stirred" although this may be the case often in practice. Column length (normalised) is here brought out as a design parameter in both cases whereas this has not been done for the CSTC representation in the past.

A purpose in considering both types of model is to ascertain in detail the extent to which a CSTC representation might be used as an approximation to the more difficult tubular process for the purpose of design simplification.

Section 2 deals with large-signal steady state behaviour. Small signal dynamic behaviour is derived in Section 3. Control aspects are considered in Section 4.

The report is confined to packed columns. Tray type columns will be considered in a later report.

2 Large Signal Behaviour

2.1. Tubular Column

2.2.1. Large Signal PDE Model

Following Edwards [1] and introducing his inverted U-tube concept at the outset, such that setting distance $h' = 0$ locates the accumulator and reboiler end vessels whilst h'=L' fixes the feed position, then the following pde's describe the

behaviour of vapour-and liquid-compositions (as mol-fractions) Y(h',t) and X'(h',t) respectively within the upper (rectifying) and lower (stripping) sections of the distillation column:

$$\frac{\partial Y}{\partial \tau} - \frac{V_r}{k}\frac{\partial Y}{\partial h'} = Y_e - Y = -\frac{\partial Y_e}{\partial \tau} - \frac{\alpha L_r}{k}\frac{\partial Y_e}{\partial h'} \qquad (1)$$

and $$\frac{\partial X'}{\partial \tau} - \frac{L_s}{k}\frac{\partial X'}{\partial h'} = X_e' - X' = -\frac{\partial X_e'}{\partial \tau} - \frac{\alpha V_s}{k}\frac{\partial X_e'}{\partial h'} \qquad (2)$$

where normalised time $\tau = t / T_n$ (3)

and base time $T_n = H / k =$ constant (4)

The model assumes the constant molar vapour and liquid capacitanes p.u. length are symmetrically related thus:

$$H_{rv} = \alpha H_{sv} = \alpha H_{rl} = H_{sl} = H \qquad (5)$$

where suffixes r and s denote rectifier and stripper whilst l and v denote liquid and vapour. The parameter α (>1.0) is related to the relative volatility ,β, of the binary mixture and the equilibrium relationship{i.e. $\beta = Y_e(1-X)/X(1-Y_e) = Y'(1-X_e')/X_e'(1-Y')$}, is approximated by piecewise linear relationships for rectifier and stripper thus

$$1 - Y_e = \alpha(1 - X) \qquad \text{(for the rectifier)} \qquad (6)$$

and $$Y' = \alpha X_e' \qquad \text{(for the stripper)} \qquad (7)$$

It is further assumed that column and packings are designed such that the rectifier and stripper evaporation constants k_r and k_s expressed as evaporation rates p.u. length p.u. departure from equilibrium (Y_e-Y and X'-X_e' respectively) are constant and equal; i.e.:

$$k_r = k_s = k \qquad (8)$$

Flow rates Vr, Lr, Vs and Ls and denote the bulk flows of vapour and liquid up and down the column, suffixes r and s again denoting the rectifier and stripping zones.

2.1.2 Steady-state Equations for Symmetrical Operation

If we operate the column such that quiescently

$$V_r = \alpha L_r = L_s = \alpha V_s = V \qquad (9)$$

then, setting normalised distance h such that

$$h = h' / L_n \qquad (10)$$

where base distance $L_n = V / k$ (11)

the simple subtraction of equation (2) from (1) yields, in steady state, the simple separation equations:

$$\frac{dS}{dh} = S - S_e = \frac{dS_e}{dh} \qquad (12)$$

where $S(h) = Y(h) - X'(h)$ (13)

and $S_e(h) = Y_e(h) - X_e'(h)$ (14)

[Note that a decoupled pair of equations for total compositions Y+X' and Y_e+X_e' could also be written down by adding (1) and (2)]

2.1.3 Boundary Conditions

The feedpoint boundary equations may be written (in general)

$$V_s\alpha X_e'(L') + F_v z = V_r Y(L') \tag{15}$$

and $$L_r\{1-\alpha+\alpha Y_e(L')\} + F_l Z = L_s X'(L') \tag{16}$$

Now as vapour feed flow $$F_v = V_r - V_s \tag{17}$$

and liquid feed flow $$F_l = L_s - L_r \tag{18}$$

and if feed liquid composition $$Z = 1/(1+\alpha) \tag{19}$$

whilst feed vapour composition $$z = \alpha/(1+\alpha) \tag{20}$$

(so that the feed is in equilibrium at the knee of the linearised equilibrium curve) then, under the assumed symmetrical quiescent operating conditions (9), the separation boundary condition at the feed point reduces to simply:

$$S(L') - S_e(L') = 2\varepsilon/(\alpha+1) \tag{21}$$

where $$\varepsilon = \alpha+1 \tag{22}$$

The end vessel boundary conditions involve accumulator and reboiler capacitances (made equal here at H_e) and are therefore differential equations rather than algebraic equations in general (unlike the feed point equations above). They are

$$H_e\alpha\dot{Y}_e(0) = V_r[\alpha\{1-Y_e(0)\} - \{1-Y(0)\}] \tag{23}$$

and $$H_e\alpha\dot{X}_e'(0) = L_s[X'(0) - \alpha X_e'(0)] \tag{24}$$

However, under the assumed operating conditions, in steady-state, we get simply:

$$\alpha S_e(0) - S(0) = \varepsilon \tag{25}$$

2.1.4 Steady State Solution

Assuming a linear solution (in h):

$$S = -2Gh + C_1 \tag{26}$$

so that $$S_e = -2Gh + C_2 \tag{27}$$

where G, C_1 nd C_2 are constants, by substitution in (12),(21) and (25) we derive

$$G = \frac{2\varepsilon}{(\alpha+1)(2\varepsilon L+\alpha+1)} \tag{28}$$

and $$S(0)\ [=C_1] = \frac{\varepsilon\{\varepsilon+2(\alpha+1)L\}}{(\alpha+1)(2\varepsilon L+\alpha+1)} \tag{29}$$

We thus have a simple formula for the separation S(0) {=Y(0)-X'(0)}between the composition of the vapour produced at the top of the tubular column and that of the liquid at the bottom in terms of parameter α and L (ε=α-1): i.e. in terms of α and real column length L', evaporation parameter k and quiescent operating vapour flow V,

since L=L'k/V. The implications of formula (29) are postponed until after the next subsection (2.2) devoted to the CSTC column.

2.2. CSTC Column

2.2.1 Large signal DE's

In this case the rectifier vapour composition is lumped in a single zone as Y(0) and the stripper liquid composition as X'(0). $Y_e(1)$ denotes the vapour composition that exists in equilibrium with accumulator liquid composition X(1) whilst $X_e'(1)$ is the liquid composition in equilibrium with vapour composition Y'(1) produced by the roboiler. The same equilibrium relationships (6) & (7) are assumed to apply generally as for the tubular model. Following Tabrizi and Edwards [2] but using symbols k_r and k_s here as in Section 2.1 to denote evaporation rates p. u. length and L' again to denoted section length (i. e. k_rL', k_sL' here≡k_r, k_s in Tabrizi). Under the same physical symmetry assumptions (5) and (8) as for tubular models, again using τ to denote normalised time t/T_n and where T_n is given by (4), then if $\dot{q}$ denotes $dq/d\tau$, the rectifier and stripping section mass balances can be written compactly thus:

$$\dot{Y}(0)+\frac{V_rY(0)-\alpha V_sX_e'(0)-F_vz}{kL'}=Y_e(0)-Y(0)=-\dot{Y}_e(0)-\frac{\alpha L_r\{Y_e(0)-Y_e(1)\}}{kL'} \qquad (30)$$

and

$$\dot{X}'(0)+\frac{L_sX'(0)-\alpha L_rY_e(0)+(\alpha-1)L_r-F_lZ}{kL'}=X_e'(0)-X'(0)=-\dot{X}_e'(0)-\frac{\alpha V_s\{X'_e(0)-X_e'(1)\}}{kL'}$$

(31)

2. 2. 2. Terminal Boundary DE's

The feed boundary equations and those for the rectifier and stripping sections (above) are synonymous but the end vessels again introduce additional DE's due to their separate capacitances. There are:

$$H_a\alpha\frac{dY_e(1)}{dt}=V_r\{Y(0)-\alpha Y_e(1)-\alpha+1\} \qquad (32)$$

and $$H_b\frac{dX_e'(1)}{dt}=L_s\{X'(0)-\alpha X_e'(1)\} \qquad (33)$$

2.2.3. Steady-State Equations under Symmetrical Operation

Assuming the balanced flow conditions of eq[n]. (9) and a feed mixture in equilibrium at the knee of the linearised equilibrium curve of eq[n]s (19) & (20) (i. e., exactly as for the tubular column) then

$$F_lZ-F_vz-(\alpha-1)L_r=\frac{(1-\alpha)}{(1+\alpha)}\frac{(\alpha-1)V}{\alpha}-\frac{\alpha-1}{\alpha}V=-\frac{2(\alpha-1)V}{(\alpha+1)} \qquad (34)$$

so that subtracting eq[n](31) from (30) in steady we get the large-signal separation equation:

$$\frac{S(0)-S_e(0)-2\varepsilon/(\alpha+1)}{L}=S_e(0)-S(0)=\frac{S_e(1)-S_e(0)}{L} \qquad (35)$$

where again normalised length $L=L'/L_n$ and $L_n=V/k.$,

Here $$S = Y - X' \tag{36}$$

Whilst $$S_e = Y_e - X_e' \tag{37}$$

[Again a decoupled equation for <u>total</u> composition rather than separation therein could be written in addition to (35) (by adding (30) and (31)) but this is not of interest in a report confined to separation dynamics]

The terminal boundary conditions (32) and (33) subtract in steady state, under the same operating conditions (9), to give:

$$\alpha S_e(1) - S(0) = \varepsilon \tag{38}$$

2.2.4. <u>Steady State Solution</u>

Eliminating $S_e(1)$ using eq^n (38) we get:

$$S_e(0) = \frac{\varepsilon + S(0)(L\alpha + 1)}{\alpha(L+1)}$$

and also $$S_e(0) = \frac{S(0)(L+1) - 2\varepsilon/(\alpha+1)}{(L-1)}$$

from which we obtain the CSTC column separation:

$$S(0) = \frac{\varepsilon}{(\alpha+1)}\left[\frac{(3\alpha+1)L + \alpha - 1}{(3\alpha-1)L + \alpha + 1}\right] \tag{39}$$

The differences and similarities in steady-state separation characteristics predicted by the two models (29) and (39) is explored in the next Section 2.3.

2. 3 <u>Comparison of Steady State Separation Characteristics of the Tubular and CSTC Column Models</u>

2. 3.1. <u>Comparison of Separation Surfaces</u>

The steady state separations for packed column have been deduced as in terms of L and α (a), for the tubular column as:

$$S = S(0) = \frac{\varepsilon}{(\alpha+1)}\left[\frac{2(\alpha+1)L + \varepsilon}{2\varepsilon L + \alpha + 1}\right] \tag{40}$$

and (b), for the CSTC column as:

$$S = S(0) = \frac{\varepsilon}{(\alpha+1)}\left[\frac{(3\alpha+1)L + \varepsilon}{(3\alpha-1)L + \alpha + 1}\right] \tag{41}$$

where $$\varepsilon = \alpha - 1 \tag{42}$$

and $$L = Lk/V \tag{43}$$

The argument h=0 is now dropped for convenience and the variable S will now be understood to apply to the separation of composition between top and bottom of the column.

Plotted as a function of plant parameters L and α , the S-surface, i.e. $S(L,\alpha)$ for each of the two cases is graphed in Figs 1 & 2 respectively. For any given α, the

RHS of equations (40) & (41) intersect only at L=0 and, for any given L, α combination, the separation produced by the tubular column exceeds that generated by the CSTC. This is as might be expected since the tubular column acts as a sequence of infinitesimal CSTC'S each feeding its neighbour with a progressively enriched (depleted) feed mixture via the circulating vapour (liquid) streams as we move from the column feed point, at h=L, towards the accumulator (reboiler), at h=0, along the rectifier (stripping section). Thus, as can be seen from eq^n. (40),

for the tubular column, $$\underset{L\to\infty}{Lim} \mid S = S_m = 1.0 \qquad (44)$$

whereas, for the CSTC, $$\underset{L\to\infty}{Lim} \mid S = S_m = \frac{\varepsilon(3\alpha+1)}{(\alpha+1)(3\alpha-1)} \qquad (45)$$

Thus, the value of S can be raised arbitrarily towards unity (i. e. Y(0)=1.0 and X'(0)=0.0), no matter what the value of feed parameter α (>1.0), merely by increasing design parameter L. i.e. by increasing real lengthen L', increasing evaporation parameter k of the packing material, or by decreasing the quiescent circulating flow V at which the plant is operated. Increasing L by either of these means will also increase the value of separation produced by the CSTC for a given α (>1.0) but only towards asymptotic values, S_m<1.0, set by α and given by eq^n .45. The value of S_m increases with α but so too does the value of S_f : the initial separation z-Z of the feed mixture since from eq^{n}s(19) and (20),

$$S_f = \varepsilon / (\alpha+1) \qquad (46)$$

Clearly the potential improvement in separation

$$\underset{\alpha\to\infty}{Lim}(S_m - S_f) = 0.0 \qquad (47)$$

i. e. the potential improvement becomes progressively less as the volatility of the feed mixture increases even though (for the CSTC) S_m also increases with α.

2. 3. 2. Important Note on the Effect of Changing V at the Plant Design Stage

We have noted above that S may be increased by increase of L through, say, a reduction in quiescent vapour flow V. This is counter-intuitive at first sight since one would expect greater separation to by achieved by increasing the boiling (and condensing) rate i. e. by increasing the energy throughput. This expectation assumes a given material throughput F_l+F_v however which contravenes our design assumption V_r=αL_r=αV_s=L_s=V (eq^n 9) from which follows:

$$F_v = F_l = D = W = V\varepsilon / \alpha \qquad (48)$$

where D and W denote output flow rates of top and bottom product from the column (i. e. from the accumulator and reboiler before recycling the remaining flow). Fig 3 summarises the quiescent flow conditions in the column. Design equation (9) was imposed to ensure even loading across the column (i. e. constant composition gradient G in the tubular case) and resulting equation (48) requires that, if V is reduced, then so too must be the feed and product take-off rates F_v, F_l, D & W . Thus reduced material throughput is implied at the design stage. Intuition is now satisfied since increase in S is effectively accomplished by reduction in steady-state material throughput as well as

by simultaneously reduced energy flow. If the material throughput rate is pre-specified then, for a given α, V is fixed by eqn (48) i. e. by (9) and be separation can only be modified by choice of length L' or evaporation constant k.

All this is at the design stage when quiescent levels are decided upon. This does not prevent subsequent perturbation of input variables V and L (despite given feed flows) in order to control S in the neighbourhood of its steady-state design value. Such control implies small departures from the design condition (9) (whilst respecting input & output flow balance conditions) and by this means and under these circumstances, it will be shown in Section 3 that an increase of V (and L) can increase S, (F_v, F_l, D & W remaining constant meanwhile). As stated, intuition is thus satisfied.

2.3.3. Constant Separation Loci

From a column design viewpoint, the separation formulae (40) and (41) are better expressed in the form $L(S,\alpha)$ rather than $S(L,\alpha)$. This is because the input parameters to the column designer are feed specification α and column performance specification S. At the column design stage, plant parameter L is a dependent variable to be deduced * . For the tubular column, the relevant equation (40) readily rewritten thus

$$L = \frac{S(\alpha+1)^2 - (\alpha-1)^2}{2(1-S)(\alpha-1)(\alpha+1)} \qquad (49)$$

which applies to all $\alpha>1.0$ and to

$$(\frac{\alpha-1}{\alpha+1})^2 < S < 1.0 \qquad (50)$$

Constraint (50) is trivial practically since the feed separation $S_f=(\alpha-1)/(\alpha+1)$ so that the lower limit of (50) pertains to S < feed separation: Clearly this condition has no practical relevance. Clearly $L\rightarrow\infty$ for $1.0<\alpha\rightarrow\infty$ which would be expected since a mixture of $\alpha=1.0$ is undistillable. L is asymptotic to -0.5 as $\alpha\rightarrow\infty$, becoming negative only for α contravening constraint (50). Constant separation loci of L versus α are shown in Fig 4. Fig 5 shows S versus L for selected values of α computed from eq^n.(40)

For the CSTC column, separation equation (41) may be rewritten for $L(S,\alpha)$ thus:

$$L = \frac{S(\alpha+1)^2 - (\alpha-1)^2}{(3\alpha+1)(\alpha-1) - S(\alpha+1)(3\alpha-1)} \qquad (51)$$

and applies practically within the limited α- range

$$\frac{S+1+2\sqrt{S^2-S+1}}{3(1-S)} < \alpha < \frac{S+1+2\sqrt{S}}{1-S} \qquad (52)$$

---

* The situation is different in the plant "rating" exercise where L and α are then the given inputs and the expected separation performance from the existing plant is to be evaluated.

The lower limit corresponds to $S \rightarrow S_m$ (i. e. $L \rightarrow \infty$) and the upper to $L>0$. Outside this range of α the constraint $1.0<\alpha$ and $L>0$ is not satisfied. As $\alpha \rightarrow \pm\infty$, L becomes asymptotic to -0.333: Of mathematical interest only! Constant separation loci of L versus α for the CSTC column, computed from (51), within range (52), are shown in Fig 6. Fig 7 shows S versus L for selected values of α.

The obvious conclusion from comparing Figs 4 and 6 or 5 and 7 is that the tubular column can separate mixtures to any extent, $S<1.0$, no matter how small α (>1.0) merely by appropriate choice of L. It is therefore well suited to difficult separations, i. e. to low α feed mixtures. By contrast, the CSTC, whilst showing the trend to increasing S with increase of L (for a given α) is capable only of a bounded range of S . The smaller the feed separation the less the potentially attainable output separation, irrespective of L. The CSTC only provides a reasonable improvement in separation for a moderate range of α.

For comparison purposes in Figs 8 and 9, lines of feed separation $S_f\{=\varepsilon/(\alpha+1)\}$ are also indicated on curves of S versus α for selected values of L for tubular and CSTC columns respectively. These curves indicate that $S>S_f$ for all L at any α in the case of the tubular column. In the case of the CSTC column, $S>S_f$ at any given α provided $L>1$.

2. 3. 4. Matching Separations of Tubular CSTC Columns

It would be useful to find that CSTC column which is, in some sense, equivalent to the tubular column. One criterion for matching the two types could be equality of steady-state separation for a given feed mixture. Accordingly we can equate $S(\alpha,L)$ given by eq^n . (40) for a tubular column of normalised length L to $S(\alpha, L_1)$ given by eq^n. (41) for a CSTC of normalised length L_1. This exercise produces the result

$$L_1 = -L/(L-1) \qquad (53)$$

i. e. $$L = L_1/(L_1+1) \qquad (54)$$

It is noteworthy (a) that this result is independent of α and (b) that matching is possible only for the condition

$$L<1.0 \qquad (55)$$

Note again however that since feed separation

$$S_f=z-Z=\varepsilon/(\alpha+1)$$

then, for the tubular column, eq^n. (40) predicts that $S>S_f$ (i. e. the column is only useful) for $L>0.5$. Hence tubular columns of normalised length

$$0.5<L<1.0 \qquad (56)$$

are the only ones that can match CSTC columns, and from eq^n. (53), the latter can occupy the normalised length range

$$1.0<L_1<\infty \qquad (57)$$

Thus from both separation formulae we deduce that matching is possible only within the limited range if separations:

$$\varepsilon/(\alpha+1)(=S_f)<S<(3\alpha+1)\varepsilon/\{(3\alpha-1)(\alpha+1)\} \qquad (58)$$

For various α, the values of the S-ranges are therefore as follows:

α=2	0.333<S<0.467
α=3	0.500<S<0.625
α=4	0.600<S<0.709
α=5	0.667<S<0.762

Thus the separation range over which matching is possible is rather restricted and is appropriate only to relatively high volatility feeds. The tubular column can handle α's down to near unity (i. e. $\varepsilon<<1.0$) and still produce output separation $\rightarrow$ 1.0 , merely by choice of L. Not so CSTC columns.

As an example, for α=3, and S=0.6, equation (49) predicts the need for a tubular column of length L=0.875. However, equation (51) (or 53) predicts L_1=7.0 i. e. $L_1>>$ L!

Finally it should be noted that separation matching can be achieved for columns of the same length L by fictitious adjustment of feed volatility in the CSTC. Setting this again to α in the tubular case but α_1 in the CSTC gives equal separations if the following formula {derived from eq^{n}s (40) and (41)} is satisfied. viz:

$$2L^2\alpha_1(\alpha^2-1)+L(3\alpha\alpha_1+1)(\alpha-\alpha_1)+(\alpha\alpha_1-1)(\alpha-\alpha_1)=0 \qquad (59)$$

This is readily verified for the case of say S=0.508, L=5.0 for which α must be 1.225 or α_1=2.400 (as the separation formulae confirm.) Eq^n. (59) has yet to be modified (if possible) to obtain $\alpha_1(L,\alpha)$ explicitly. There will be constraints on the applicability of the formula.

3. Small Signal Dynamic Behaviour

3.1. CSTC Model

3.1.1 Derivation of Transfer Function relating Separation to Circulating Flow

The model will be true, strictly, only for infinitesimal changes in the process variables around the quiescent operating point which is assumed to be governed by the design criteria of symmetry and even-loading previously set out. If prefix "d" indicates such a change in its associated variable then let

δ	denote	$dS(0)$
δ_e	denote	$dS_e(0)$
$\delta_e(1)$	denote	$dS_e(1)$
υ	denote dV_r and dV_s , F_υ and F_l being kept constant.	
l	denote dL_r and dL_s , F_υ and F_l being kept constant.	

$f=\upsilon+l$

y denotes dY, x' denotes dX'...etc.

Thus, differentiating the original dynamic balance equations (30) and (31) for the CSTC (i. e. before the symmetrical operation and other design constraints are imposed), subtracting and using p to denote d/dτ (i. e. Laplace transforming in p with respect to normalised time τ) we get :

$$\begin{aligned} & p\delta + \frac{V}{kL'}(\delta + \delta_e) + \frac{\upsilon[Y(0) - \alpha X_e'(0)]}{kL'} - \frac{l[X'(0) - \alpha Y_e(0)]}{kL'} - \frac{\varepsilon l}{kL'} \\ & = \delta_e - \delta \\ & = -p\delta_e - \frac{V}{kL'}[\delta_e - \delta_e(1)] - \frac{\alpha l[Y_e(0) - Y_e(1)]}{kL'} + \frac{\alpha\upsilon[X_e'(0) - X_e'(1)]}{kL'} \end{aligned} \tag{60}$$

In eq^n (60) and subsequent small signal equations, the remaining large signals V,Y(0), $X_e'(0)$ can be regarded as constants=the quiescent steady-state values governed by the steady-state equations derived in Section 2, thus yielding a linear model in the small perturbation δ, ν, l etc. If, as in previous analyses, for symmetry we set

$$H_a = H_b / \alpha = H' \tag{61}$$

than the small signal boundary equations (32) and (33) yield similarly:

$$p'H'\alpha\delta_e(1) = V[\delta - \alpha\delta_e(1)] + \upsilon[Y(0) - \alpha Y_e(1) + \varepsilon] - l[X'(0) - \alpha X_e'(1)] \tag{62}$$

where p' denotes d/dt. Hence:

$$\alpha[1 + \frac{p'H'}{V}]\delta_e(1) = \delta + \frac{1}{V}[\upsilon\{Y(0) - \alpha Y_e(1) + \varepsilon\} - l\{X'(0) - \alpha X_e'(1)\}] \tag{63}$$

Now if we confine attention to perturbations ν+l only , i.e. in total circulating flow, f ,whilst keeping top and bottom product flows D and W constant (i. e. ν-l=0) then

$$\upsilon = l = f / 2 \tag{64}$$

So that eq^n (60) reduces to simply

$$\begin{aligned} & p\delta + \frac{V}{kL'}(\delta + \delta_e) + \frac{f[S(0) + \alpha S_e(0)]}{2kL'} - \frac{\varepsilon f}{2kL'} = \delta_e - \delta \\ & = -p\delta_e - \frac{V[\delta_e - \delta_e(1)]}{kL'} - \frac{\alpha f[S_e(0) - S_e(1)]}{2kL'} \end{aligned} \tag{65}$$

whilst boundary condition (63) becomes

$$\delta_e(1) = \frac{1}{\alpha[1 + Tp]}[\delta + \frac{f}{2V}\{S(0) - \alpha S_e(1) + \varepsilon\}] \tag{66}$$

where T is the normalised time constant of the end vessels, i. e.:

$$T = H' / VT_n \tag{67}$$

at the quiescent rectifier vapour rate V.

The large signal steady-state relationships derived in Section 2 for the CSTC may now be used to simplify and combine eq^{n}s (65) and (66). In particular, recalling

$$L = L' / L_n = L'k / V \tag{68}$$

and eq^{n}(s) (38) et seq., rewritten here

$$S(0)-\alpha S_e(1)+\varepsilon=0 \tag{69}$$

and $$S(0)+S_e(0)-2\varepsilon/(\alpha+1)=L[S_e(0)-S(0)]=S_e(1)-S_e(0) \tag{70}$$

we can write eq^{n} (65) as

$$\begin{aligned} &pL\delta+\delta+\delta_e+\frac{u}{2}[S(0)+\alpha S_e(0)-\varepsilon]=L[\delta_e-\delta] \\ &=-pL\delta_e+[\delta_e(1)-\delta_e]+\frac{u}{2}\alpha[S_e(1)-S_e(0)] \end{aligned} \tag{71}$$

and eq^{n} (66) simply as

$$\delta_e(1)=\delta h_e(p)/\alpha \tag{72}$$

where $$h_e(p)=1/(1+Tp) \tag{73}$$

and $$u=f/V \quad \{=(\upsilon+l)/V\} \tag{74}$$

Eq^{n}.(71) can be simplified using eq^{n}s (69) and (70) if we first write

$$A=\frac{S(0)+\alpha S_e(0)-\varepsilon}{2} \tag{75}$$

$$\therefore \qquad B=\frac{S_e(1)-S_e(0)}{2} \tag{76}$$

and $$\delta\,[L+PL+1]=\delta L+\delta_e(1)+B\alpha u \tag{77}$$

giving

$$pL\delta+\delta+\delta_e+Au=L[\delta_e-\delta]=-pL\delta_e+[\delta_e(1)-\delta_e]+B\alpha u \tag{78}$$

$$\therefore \quad \delta_e[L-1]=\delta(pL+1+L)+Au$$

and $$\delta_e[L+pL+1]=\delta L+\delta_e(1)+B\alpha u$$

so that, eliminating unwanted variable δ_e and using eq^{n} (72) to remove $\delta_e(1)$, in favour of the wanted output variable δ, we get the 3rd order transfer function:

$$g_1(p)=\frac{\delta}{u}=\frac{[(L-1)B\alpha-(pL+1+L)A]}{[(pL+L+1)^2+(1-L)(L+h_e\alpha^{-1})]} \tag{79}$$

From eq^{n}s (69), (70) and (76), straightforward algebra shows quasi-constant parameters A and B to be given in terms of α and L by:

$$A=\frac{\varepsilon\{\varepsilon+(\alpha+1)L\}}{(\alpha+1)\{(\alpha+1)+(3\alpha-1)L\}} \tag{80}$$

and $$B=\frac{2\varepsilon L}{(\alpha+1)\{(\alpha+1)+(3\alpha-1)L\}} \tag{81}$$

3.1.2 Note on Symbolic Equivalence Between Source Reference and This Report

In this report it has been necessary to make some changes to the significance of certain symbols common to both this report and the source CSTC reference [2]. This

has been necessary in order that symbols have the same meaning for tubular and CSTC column. This situation did not pertain exactly to the original tubular [1] and CSTC [2] references. The definitions in reference [1] have been retained here.

The transfer-function $g_1(p)$ is identical to the version (eq^n 58) given in the original paper [2] inspection of which readily shows that the following parameter symbols are equivalent:

Table of equivalent symbols

Tabrizi and Edwards [2]	Present Report
k	kL'
a	L
p	pL
R	A
S	Bα

In Tabrizi & Edwards [2] a=k/V (=kL'/V=L in the symbolism of the present paper). The symbol τ in Tabrizi is t/T_n where T_n there=HL'/V if H is taken to be capacitance pu length as here. In this report T_n=HL'/kL'=H/k in the present symbols. Thus τ (in Tabrizi)$\equiv\tau$(here)$\times$V/(kL')=τ/L (here). Hence p (in Tabrizi)$\equiv$pL (here)

3. 1. 3. CSTC Column: Gain, Transfer Function and Frequency Response

In principle the transfer function for the CSTC column can be evaluated in terms of just p and the key parameters L, α and T from eq^n (79) by using eq^n.s (80) and (81) to eliminate algebraic quantities A and B. The resulting analytic expression for the third-order transfer function would be cumbersome and not particularly enlightening without subsequent analysis of its asymptotic behaviour as $|p| \to 0$ and ∞. For the special case of T=0 (for end-vessels if negligible capacitance), i. e. making

$$h_e(p) = 1.0 \qquad (T = 0) \tag{82}$$

reduces $g_1(p)$ to the simple second order form:

$$g_1(p) = \frac{\alpha\varepsilon}{(\alpha+1)}\left[\frac{\varepsilon L^2 - 4\alpha L - \varepsilon - pL\{\varepsilon + (\alpha+1)L\}}{\{\alpha+1+(3\alpha-1)L\}[\alpha+1+(3\alpha-1)L+2\alpha(L+1)Lp+\alpha L^2p^2]}\right] \tag{83}$$

The static gain $g_1(0)$ is, of course, independent of T in general, since $h_e(0)$=1.0, so this may be deduced from (83) simply by setting p=0, giving:

$$g_1(0) = \frac{\alpha\varepsilon}{(\alpha+1)}\left[\frac{\varepsilon L^2 - 4\alpha L - \varepsilon}{\{\alpha+1+(3\alpha-1)L\}^2}\right] \tag{84}$$

which will be positive for longer columns, i. e. which satisfy the condition:

$$\varepsilon L^2 > 4\alpha L + \varepsilon \tag{85}$$

but whose sign is clearly parameter sensitive and we note the possibility of zero gain, i.e.:

$$g_1(0)=0.0 \qquad \text{if} \qquad \varepsilon L^2 = 4\alpha L + \varepsilon \tag{86}$$

Substantial positive gain (i. e. greater separation for greater circulating flow at a given throughput) will be an important design goal presumably. This is discussed later.

The asymptotic behaviour of $g_1(p)$ as $|p| \to 0$ and ∞ involves dynamic terms for which eq^n (83), being only a special case, (i. e. for T=0) is inadequate as a source of derivation. Instead we must return to the general form of eq^n (79), retaining the general end-vessel model:

$$h_e(P) = 1/(1+T_p) \tag{87}$$

Doing this, retaining only the two smallest powers of p in the numerator and denominator as $|p| \to 0$ and approximating their ratio accordingly shows that, in general, $g_1(p)$ tends to a first order lag as $p \to 0$ of the form

$$\lim_{|p|\to 0} g_1(p) = \frac{g_0}{1+T_0 p} \tag{88}$$

where $g_0 = g_1(0)$ (89)

$$T_0 = \frac{2\alpha L(L+1)+T(L-1)}{(3\alpha-1)L+\alpha+1} + \frac{L\{\varepsilon+(\alpha+1)L\}}{\varepsilon L^2 - 4\alpha L - \varepsilon} \tag{90}$$

[The special case for T=0 is readily confirmed by approximating the expression for $g_1(p)$ in eq^n (83) by considering only powers of $p=p^0$and p^1 in the numerator and denominator]

Turning attention to high frequency behaviour, a similar approach but retaining only the powers p^1 and p^0 in the numerator and p^2 and p^1 in the denominator of eq^n (79) yields

$$\lim_{|p|\to\infty} g_1(p) = \frac{-g_\infty}{1+T_\infty p} \tag{91}$$

where $$g_\infty = \frac{\varepsilon\{\varepsilon+(\alpha+1)L\}^2}{(\alpha+1)\{\alpha+1+(3\alpha-1)L\}\{\varepsilon+(3\alpha+1)L^2\}} \tag{92}$$

and $$T_\infty = \frac{L\{L(\alpha+1)+\varepsilon\}}{\{L^2(3\alpha+1)+\varepsilon\}} \tag{93}$$

[g_∞ and T_∞ are independent of T since this parameter does not affect the coefficients of the highest two powers of p in $g_1(p)$, and eq^n. s (91) the (93) could have been derived directly from the special case eq^n. (83)]

The important feature to note is that, for $g_1(0)>0$, the asymptotic model at low frequency is a first-order lag of <u>positive</u> gain (and time constant) provided L>1 of course. The asymptotic model at high frequency is a different first order lag but this time of <u>negative</u> gain (=$-g_\infty$). The process therefore has nonminimum-phase properties. Its inverse Nyquist locus starts vertically into quadrant 1 from the real axis at $g_1(0)^{-1}$, encircles the origin and approaches $-j\infty$ vertically downwards in quadrant 3. Its step response will begin negatively as that of the system $-g_\infty/(1+T_\infty p)$ but finish positively as that of $g_0/(1+T_0 p)$.

3.2 <u>Tubular Column Model</u>

3. 2. 1. <u>Transfer Function Relating Separation to Circulating Flow</u>

As with the CSTC model, it is possible to segregate the small signal equations (this time pde's) pertaining to separation change y-x' (=δ) from those relating to the change y+x' when the column is operated symmetrically. Derivation of the transfer function relating δ to circulating flow change v+l can then proceed separately to that relating y+x' to v+l on similar lines. The derivation is not presented here but the result is the same* as that presented in the cited reference (1). The derived transfer function is :

$$\frac{\delta}{u} = g_1(p) = G[\frac{\varepsilon(\cosh qL - 1)/p - (1+\alpha)(\sinh ql)/q - \varepsilon/2}{(1-h_e\alpha^{-1})(\sinh qL)q/p + (1+h_e\alpha^{-1})\cosh qL}] \quad (94)$$

where $$q^2 = p(p+2) \quad (95)$$

Input u is defined as for the CSTC case (eqn. 74)

i. e. $$u = f/V = (\upsilon + l)/V \quad (96)$$

and steady state composition gradient G is as defined in eqns (26) and (28).

Despite the hyperbolic functions in eqn. (94), inverse Nyquist loci $g_1^{-1}(j\omega)$ can be derived, computed and plotted as shown in (1). As demonstrated in Section 3. 2. 2, the asymptotic behaviour of such loci is also predictable by considering limits of $g_1(p)$ as $|p| \to 0$ and ∞ . This behaviour bears some resemblance to the CSTC model behaviour already predicted by a similar process

3. 2. 2. Tubular Column: Gain and Asymptotic Frequency Response

As $p \to 0$ i. e. as $qL << 1.0$, sinh qL may be approximated by qL and cosh qL by $1 + p^2L^2/2$ so that provided terminal capacitance T is not excessive (i. e. non-dominant) then it is readily shown, by approximating eqn (94), that

$$\lim_{|p|\to 0} g_1(p) = G\alpha[\frac{\{\varepsilon L^2 - (1+\alpha)L - \varepsilon/2\} + \varepsilon L^2 p/2}{(2\varepsilon L + \alpha + 1) + p\{\varepsilon L + (\alpha+1)L^2\} + p^2(\alpha+1)L^2/2}] \quad (97)$$

The steady state gain $g_1(0)$ is clearly given by

$$g_1(0) = \frac{G\alpha\{\varepsilon L^2 - (1+\alpha)L - \varepsilon/2\}}{2\varepsilon L + \alpha + 1} \quad (98)$$

or, substituting our derived parametric solution (28) for gradient G,:

$$g_1(0) = \frac{2\alpha\varepsilon\{\varepsilon L^2 - (1+\alpha)L - \varepsilon/2\}}{(\alpha+1)(2\varepsilon L + \alpha + 1)^2} \quad (99)$$

The two gain formulae (84) and (99) (for the CSTC and tubular column respectively) though different, have clearly some strong similarities. In particular we note again that $g_1(0)$ for the tubular column will be positive for longer columns, this time for a slightly different condition compared to (85), viz:

$$\varepsilon L^2 > (1+\alpha)L + \varepsilon/2 \quad (100)$$

---

* Note that in the source reference (1), the symbol $g_1(p)$ is defined as (y-x')V/G(v+l) whereas here it is defined as $\frac{\delta}{u}(= \frac{(y-x')V}{(v+l)})$. Hence the G term in eqn (94) not appearing in ref. (1).

The realistic possibility of negative gain also exists however and indeed zero gain, i. e.:

$g_1(0)=0$ if $\varepsilon L^2 = (1+\alpha)L+\varepsilon/2$ (101)

Again, however, a positive $g_1(o)$ will be a design goal by suitable choice of L provided this does not conflict with the specification for steady-state (large-signal) separation S(0) (eq^n. 29)

The low frequency asymptotic transfer function (97) again reduces to a transfer function of the form

$$\lim_{|p|\to 0} g_1(p) = \frac{g_0}{1+T_0 p} \qquad (102)$$

where $g_0 = g_1(0)$ (eq^n. 99) (101)

and $T_0 = \dfrac{\varepsilon L+(\alpha+1)L^2}{2\varepsilon L+\alpha+1} - \dfrac{\varepsilon L^2}{2\{\varepsilon L^2-(1+\alpha)L-\varepsilon/2\}}$ (102)

T_0 will be clearly positive for longer columns L>>1.0, even when $\varepsilon L^2 > (1+\alpha)L+\varepsilon/2$ (the g_0>0 condition) since then, L^2>L. Thus, for g_0 positive (negative), the asymptotic low frequency model is again a positive-(negative) going first-order lag as with the CSTC. [The possibility of T_0<0 for a limited range of L is not considered here and awaits further examination. Likewise the effect on T_0 of a large T.]

The asymptotic behaviour of $g_1(p)$ for the tubular column may be deduced from eq^n. (94) using the approximations as $|p|\to\infty$

$$q \to p+1 \qquad (103)$$

and $\cosh qL \to \sinh qL \to 0.5e^{qL}$ (104)

Unlike the CSTC column, in this case, the h.f. asymptotic behaviour of $g_1(p)$ is affected by whether or not T is zero. For $p>>T^{-1}$ (only possible if $T\neq 0$) then $h_e(p)\to 0$ whereas $h_e(p)$ remains=1.0 if T=0. In either case we deduce

$$\lim_{|p|\to\infty} g_1(p) = \frac{-g_\infty}{(1+T_\infty p)} \qquad (105)$$

as in the CSTC case, but here

$$g_\infty = 2G/(2+\alpha), \quad T>0 \qquad (106)$$

or $g_\infty = 2G\alpha/(\alpha+1)^2, \quad T=0$ (107)

and $T_\infty = 2/(2+\alpha), \quad T>0$ (108)

or $T_\infty = 2/(1+\alpha), \quad T=0$ (109)

The predictions confirm high and low frequency characteristics of the computed loci given in reference (1). In particular, Fig. 2.11 (b) of ref. (1) reproduced here as Fig. 12 for α=2.0 (ε=1.0) , L=5.0 and T=20, indicates a starting point $g_1^{-1}(0) = 0.565G^{-1}$, and a high frequency asymptote for $g_1^{-1}(j\omega)$ of $-(2+j\omega)G^{-1}$, i. e. g_∞=0.5G and T_∞=0.5 . Equations (98), (106) and (108) predict these values.

It should be noted that in the tubular column case, (unlike the CSTC), the h.f locus of $g^{-1}(j\omega)$ does not converge to the predicted h. f. asymptote but oscillates about it. The oscillations are excluded from the foregoing h. f. asymptotic predictions

which take no account of the complex nature of variable q when p is set=jω. However, only for short tubular columns do the oscillations in $g^{-1}(j\omega)$ become a serious control consideration since, for L>>1.0, the travelling waves (modelled by eq^n (94) but not by the asymptotic approximations) are rapidly attenuated giving only the insignificant ripples and loops evident in Fig 12.

The key observation from this analysis is the presence of non-minimum behaviour for tubular columns of positive separation-gain. In this respect CSTC and tubular columns are similar. In respect of travelling waves their behaviour differs (as would be expected since such waves are a pde phenomenon).

3. 3. Comparison of the Tubular and CSTC Column Gains

The static gains of the two types of column have been shown to be given by:

for the tubular column:

$$g_0 = \frac{2\alpha\varepsilon\{\varepsilon L^2 - (\alpha+1)L - \varepsilon/2\}}{(\alpha+1)\{2\varepsilon L + \alpha + 1\}^2} \qquad (110)$$

and, for the CSTC:

$$g_0 = \frac{\alpha\varepsilon}{(\alpha+1)}\left[\frac{\varepsilon L^2 - 4\alpha L - \varepsilon}{\{(3\alpha-1)L + \alpha + 1\}^2}\right] \qquad (111)$$

Curves of the two functions, g_0 versus L, for various values of α are shown in Figs 10 and 11 respectively. Clearly the gain of the tubular column exceeds that of the CSTC very considerably for any given combination of parameters L, α. Both sets of curves show that g_0 can be negative for lower ranges of L. Simultaneous matching of a CSTC of length L_1, and a tubular column of length L for gain and separation is not possible by manipulation of parameter L_1 at a given α since, for separation matching this is only possible in the range $0.5<L<1.0$ (i. e. $1.0<L_1<\infty$) as shown in Section 2.3.4. With L<1.0 however, the tubular column gain is always negative and therefore of little practical interest.

As $L\rightarrow\infty$, eq^n (111) predicts asymptotic gain values for the CSTC of 0.1250 for small α ($\varepsilon<<1.0$) and 0.1111 for $\alpha>>1.0$. For tubular columns, eq^n (110) predicts asymptotic gains, as $L\rightarrow\infty$, of 0.2500 for small α and 0.5000 for large α. Thus, the range of attainable gain is (a) lower, and (b) narrower for the CSTC compared to the tubular model. [The opposite effects of increasing α on the gains in the two cases is interesting.]

Matching static gains is probably not the best criterion for achieving equivalence of dynamic control characteristics, however, since a low process gain (g_0 in this application) can be always by compensated by increasing the controller gain K. What matters is the attainable open-loop gain Kg_0 { and hence closed-loop gain $Kg_0/(1+Kg_0)$ } before instability ensues. This question is pursued in the next Section.

4. Control Implications of the Models

4. 1. Fitting a Second Order System to the Asymptotic Models

For all cases examined, tubular and CSTC with or without significant end-vessel capacitance, it has been shown that the asymptotic transfer functions (at p=0 and ∞) take the form:

$$\lim_{|p|\to 0} g_1(p) = \frac{g_0}{1+T_0 p} \qquad (112)$$

and

$$\lim_{|p|\to \infty} g\ (p) = \frac{-g_\infty}{1+T_\infty p} \qquad (113)$$

Where model parameters g_∞,T_∞ and T_0 depend on process parameters L, α and T whilst g_0 depends on L and α only. For the different types of process, (tubular or CSTC) the precise relationships between the model-and process-parameters have similar mathematical structures but are not identical. [See eq^n s. (84), (90) (92) and (93) for the CSTC and (99),(102) and (106) through (109) for the tubular column].

Parameter g_0 can be negative for shorter columns of both types but is positive for longer processes. This latter is the case of practical interest to which we shall confine attention here. The other parameters are all positive either invariably or under the same conditions that g_0 is positive.

The minimal linear model that has the same asymptotic behaviour (given by eq^{n}s. 112 and 113) is

$$g_A(p) = \frac{g_0(1-T_1 p)}{1+(T_2+T_3)p+T_2T_3p^2} \qquad (114)$$

i. e.

$$g_A(p) = \frac{g_0(1-T_1 p)}{1+ap+bp^2} \qquad (115)$$

where $a = T_2 + T_3$ (116)

and $b = T_2T_3$ (117)

By matching the asymptotic behaviour of $g_A(p)$ to $g_1(p)$ it is readily shown that the parameters of $g_A(p)$ are related to those of $g_1(p)$ thus:

$$a\ (= T_1 + T_2) = \frac{g_0(T_0 - T_\infty)}{(g_0 + g_\infty)} \qquad (118)$$

$$T_1 = \frac{g_0T_\infty + g_\infty T_0}{(g_0 + g_\infty)} \qquad (119)$$

and

$$b\ (= T_2T_3) = \frac{g_0T_\infty}{g_\infty}\left[\frac{g_0T_\infty + g_\infty T_0}{g_0 + g_\infty}\right] \qquad (120)$$

For example using the parameters for the tubular column of Fig. 12 [i. e. α=2.0, (ε=1.0), L=5.0, T=20.0], using eq^{n}s. (101), (106),(102) and (108) we deduce g_0=1.77G, g_∞=0.5G, T_0=4.838 and T_∞=0.5 thus yielding the approximate transfer function

$$g_A(p) = \frac{1.77G(1-1.456p)}{1+3.382p+2.576p^2} \qquad (121)$$

The locus of $g_A^{-1}(j\omega)$ is shown in Fig 13 and clearly compares favourably with that of $g_1^{-1}(j\omega)$ shown in Fig. 12.

We have thus approximated the 3rd order CSTC model and the infinite-order tubular model by a second order model. All are nonminimum phase models (if g_0 is positive). For the special case of the CSTC with zero end capacitance (i. e. with T=0), $g_A(p)$ and $g_1(p)$ will be identical since the CSTC model itself is then only second order.

4. 2. Closed-Loop Stability Criterion based on $g_A(p)$

If a simple linear proportional controller of gain K is applied to $g_A(p)$ then the closed loop transfer function of the process will be

$$g_c(p) = \frac{Kg_0(1-T_1p)}{(1+Kg_0)+p(a-Kg_0T_1)+bp^2} \qquad (122)$$

so that for closed loop stability (i. e. for a positive closed-loop damping ratio)

$$Kg_0 < a/T_1 \qquad (123)$$

Thus from eq^{n}s (118) and (119) it follows that, for stability:

$$Kg_0 < \frac{g_0(T_0-T_\infty)}{g_0T_\infty + g_\infty T_0} \qquad (124)$$

Thus, if K_c denotes the critical value of K (i. e. for critical closed-loop stability), then

$$K_cg_0 = \frac{g_0(T_0-T_\infty)}{g_0T_\infty + g_\infty T_0} \qquad (125)$$

and the proportional control error E $\{=1/(1+Kg_0)\}$, at critical stability will be E_c, given by:

$$E_c = \frac{1}{1+K_cg_0} = \frac{g_0T_\infty + g_\infty T_0}{(g_\infty + g_0)T_0} \qquad (126)$$

Equation (126) is very important since, used in conjunction with the eq^{n}s relating g_0, g_∞, T_0 and T_∞ to L , α and T, it allows analytic prediction of the maximum attainable (proportional) control accuracy directly from a knowledge of the 3 basic process parameters, L, α and T.

4. 3. Performance Parameters for Columns of Both Types: Numerical Examples

Table 1 below sets out the steady-state quiescent and controlled performance parameters S and E_c for several processes (a)-(f) together with the intermediate parameters used in their calculation.

Cases (a) and (b) show that, for moderate α , even though L is made >>1.0 (to boost g_0 for the CSTC), the tubular column considerably outperforms a CSTC of the same source parameters in terms of both separation S and critical control error E_c.

As case (c) illustrates, a fairly drastic " shortening" of the tubular column (from L=20 to 5) at the same value of α (=2) brings about a similar control accuracy as that of the longer CSTC but the tubular separation remains considerably greater than the CSTC's. Cases (d) and (e) illustrate the comparative performance of a CSTC and tubular

column having different L and α values, but selected to give near identical separations. To achieve this, L for the CSTC remains considerably the larger (15 cf 4) and likewise α for the CSTC > the value for the tubular. This step causes the CSTC now to considerably outperform the tubular column under closed loop control and is the result of choosing parameters for the latter that approach the g_0 sign-change condition (see eq^n 101). In case (f), the normalised length of the tubular column is raised slightly (from 4 to 6) but α reduced (from 2 to 1.6) to again cause a separation S≅0.75 {as in cases (d) and (e) }. In this case E_c is much closer to the CSTC of case (d) than was case (e). It should clearly be possible to find matching L, α relationships between the two types of column that give identical values of S and Ec for the two cases. i. e. static and dynamic matching of CSTC and tubular models should be possible by fictitiously inflating parameters L and α for the CSTC. The parametric formulae involved will require careful and tedious manipulation if a possible matching criterion is to be found analytically. Computational determination should pose no problem.

Table 1. Predicted Performance Parameters for Various Columns

Case	a	b	c	d	e	f
Type	CSTC	Tubular	Tubular	CSTC	Tubular	Tubular
L	20	20	5	15	4	6
α	2	2	2	5	2	1.6
G	-	0.0155	0.05128	-	0.06061	0.07444
g_0	0.150	0.2448	0.0750	0.0426	0.03857	0.1095
g_∞	0.0043	3.445×10^{-3}	0.0114	7.567×10^{-3}	0.01347	0.02202
T_0	21.410	27.783	4.838	13.476	2.4416	13.873
T_∞	0.4356	0.500	0.500	0.3912	0.500	0.5556
$K_c g_0$	3.249	30.62	3.512	4.70	1.435	3.976
S	0.4563	0.9380	0.7948	0.7531	0.7570	0.7488
Ec %	23.54	3.16	22.16	17.54	41.10	20.10

4. 4. Towards Optimal Nonlinear Control

The control presupposed up to this point of the report has been linear and based upon a dynamic model linearised about a designed quiescent operating point. The stability and performance of such control can be predicted only in the small, and exhaustive simulation is necessary to test the range of acceptable performance within a large region of the state space. Nor has the control been designed designed to be optimal.

A recent, interesting and potentially powerful approach of Banks [3] revolves around the continuous and on-line solution of the Riccatti Equation using the currently valid A and B matrices, where A and B are state-dependent, the process being nonlinear, but its model known. The feedback coefficient matrix is thus continuously calculated, updated and applied as the measured state of the system changes. The

method has been shown to be stable in itself and to generate superior control for a range of testing examples operating over a much wider range of state space than switched linear controller can cope with. The distillation column presents a good challenge to the method inview of its bilinearity, its small-signal nonminimum phase characteristics, and its potential for local gain reversal. To facilitate testing Banks'method it is necessary first to formulate the state-dependent coefficient matrices for the state differential equation of the process. This is done here for the CSTC column:

We need a model of the form, say

$$\begin{bmatrix} \dot{S} \\ \dot{S}_e \\ \dot{S}_e(1) \end{bmatrix} = \underline{A} \begin{bmatrix} S \\ S_e \\ S_e(1) \end{bmatrix} + \underline{B} V_s + \underline{J} F \qquad (127)$$

where the separation functions S, S_e and $S_e(1)$ have their previous significance (except that here we drop the argument "0" from S(0) and Se(0)). Matrices $\underline{A}$, $\underline{B}$ and $\underline{J}$ are state dependent and yet to be found. There is only one control $V_S(t)$ if we keep perturbations υ=l (=f/2) as throughout this report. Under there circumstances, automatically:

$$L_r(t) = V_S(t) \qquad (128)$$

and

$$L_S(t) = V_r(t) \qquad (129)$$

as before but the original steady-state design equations $V_r=\alpha L_r$ and $\alpha V_S=L_S$ are not met in transient or in general. Instead, keeping $F_\upsilon=F_l=D=W=F$=constant as before, we simply have that:

$$V_r(t) = V_s(t) + F \qquad (130)$$

and

$$L_s(t) = L_r(t) + F \qquad (131)$$

Thus, subtracting eq^n (31) from (30) we get

$$\begin{aligned} &\dot{S} + \frac{V_S(S + \alpha S_e) - \varepsilon V_s + F\{S - \varepsilon/(\alpha+1)\}}{k\dot{L}} \\ &= S_e - S = -\dot{S}_e - \frac{\alpha V_S\{S_e - S_e(1)\}}{k\dot{L}} \end{aligned} \qquad (132)$$

Recalling the dot • denotes d/dτ, where again

$$\tau = t / T_n \qquad (133)$$

and

$$T_n = H / k \qquad (134)$$

and if, as before:

$$H_a = H_b / \alpha = \dot{H} \qquad (135)$$

then the boundary equations (32) and (33) yield

$$\frac{\alpha \dot{H}}{T_n} \dot{S}_e(1) = (V_S + F)\{S - \alpha S_e(1) - \varepsilon\} \qquad (136)$$

Extracting the state derivatives from eq^{n}. s (132) and (136) and recalling that normalised length L is related to k, L' and nominal rectifier vapour rate V thus

$$L = kL'/V \tag{137}$$

where $$V = \alpha F/\varepsilon = \text{ constant} \tag{138}$$

we there obtain

$$\underline{A}=\begin{bmatrix} -(1+\frac{F}{kL'}) & 1 & 0 \\ 1 & -1 & 0 \\ 0 & 0 & 0 \end{bmatrix}=\begin{bmatrix} -(\frac{L\alpha+\varepsilon}{L\alpha}) & 1 & 0 \\ 1 & -1 & 0 \\ 0 & 0 & 0 \end{bmatrix} \tag{139}$$

$$\underline{B}=\begin{bmatrix} \frac{\varepsilon - S - \alpha S_e}{kL'} \\ \alpha[S_e(1)-S_e] \\ \frac{T_n[S-\alpha S_e(1)-\varepsilon}{\alpha H'} \end{bmatrix}=\begin{bmatrix} \frac{\varepsilon - S - \alpha S_e}{LV} \\ \frac{\alpha[S_e(1)-S_e]}{V} \\ \frac{S-\alpha S_e(1)-\varepsilon}{\alpha VT} \end{bmatrix} \tag{140}$$

$$\underline{J}=\begin{bmatrix} \frac{\varepsilon}{(\alpha+1)kL'} \\ 0 \\ \frac{-T_n[S-\alpha S_e(1)-\varepsilon]}{\alpha H'} \end{bmatrix}=\begin{bmatrix} \frac{\varepsilon}{(\alpha+1)LV} \\ 0 \\ \frac{-[S-\alpha S_e(1)-\varepsilon]}{\alpha TV} \end{bmatrix} \tag{141}$$

where again T is the normalised time constant of the end vessels, viz:

$$T = H'/VT_n \tag{142}$$

Setting the LHS of (127) to zero and substituting the equations (139), (140) and (141) for <u>A</u>, <u>B</u> and <u>J</u> should, of course, produce the same steady state solutions as already derived in Section 2. 2. 4 if input V_s is again set to V-F (=V/α). The <u>dynamic</u> matrix model should now be usable in the Banks' method.

The cost function to be minimised by the real time Riccatli eq^{n} should take the form:

$$C = \int_0^\infty [(S_r - S)^2 + \lambda(\frac{\alpha V_s}{V} - 1)^2]dt \tag{143}$$

where S_r is a reference (target) separation to which the nominal rectifier vapour rate V pertains. [i. e. the parameter L in the state space model is given by L=L'k/V, and S_r and L are related by eq^{n}.(39)]. $V_s(t)$ is the control. Care will be needed not to set S_r outside the attainable range specified by eq^{n} (45). Cost weight λ that will produce an acceptable error S_r-S can be estimated from a knowledge of local gain $g_1(0)$ as indicated in Appendix 1 on the basis of equal steady-state cost rates $(S_r-S)^2$ and $\left[\lambda\frac{(\alpha V_s - V)}{V}\right]^2$. Fine tuning of λ may be important however. Results will be presented in a future report ,hopefully as a preliminary to applying the method , suitably modified, to the tubular column. The CSTC performance under the Banks controller will be compared with the linear control predictions here derived.

5. <u>Discussion and Conclusions</u>

The composition separation dynamics of CSTC and tubular symmetrical distillation columns have been examined. Unlike previous analyses [1], [2] the separation dynamics have been segregated from those pertaining to total or average product composition at an early stage of the analytic development, thus simplifying the algebra. Previously derived results for steady state product separation S and small signal transfer function $g_1(p)$ $[=(y-x')V/(v+l)]$ have been derived for both columns in terms of feed mixture volatility parameter α, normalised column length L and (in the case of $g_1(p)$), normalised end-vessel capacitance, T. However, notation is now standardised between the two types of column permitting a ready comparison and the main formulae derived are listed in Table 2 overleaf.

Although the variation of performance parameters S and $g_1(0)$ with L and α for the two columns show similar traits, numerically the two values of both S and $g_1(0)$ differ considerably between the two types. As might be expected, the tubular column out performs the CSTC significantly (for given L and α) in terms of both performance parameters.

Also derived is a second-order, nonminimum phase transfer function $g_A(p)$ that reproduces the high-and low-frequency asymptotic behaviour of both types of column. This has facilitated the formulation of a stability criterion for the maximum permissible open-loop gain $K_c g(0)$ and hence the minimum fractional closed loop error E_c $[=1/(1+K_c g(0)]$ achievable with stability. The formulae derived thus enables E_c to be evaluated for any specified α and L. Together with the S-formulae, this allows the unification of steady-state large signal design with linear controller design: An important goal of modern Chemical Engineering.

As regards the possible use of a CSTC model to mimic the behaviour of the more difficult tubular column, spot numerical substitutions of L and α in the S and E_c formulae indicate the possibility of achieving the desired match of quiescent steady-state and dynamic control by using fictitiously inflated L and α values in the CSTC model. So far however, although the $S(L,\alpha)$ formulae can be transformed into the form $L(S,\alpha)$, the $E_c(L,\alpha)$ formulae have not yet been similarly transformed analytically. Thus, whilst constant S-loci can and have been plotted from analytic formulae, constant E_c-loci formulae await derivation from the known $E_c(L,\alpha)$ function. This is a subject for further analysis, pending which constant E_c-loci may be computed from the reverse formulae here derived.

Finally, the large signal dynamic separation model for the CSTC has been formulated as a third order state equation with state-dependent coefficient matrices $\underline{A}$, $\underline{B}$ and $\underline{J}$ ($\underline{J}$ is here the disturbance coefficient matrix, $\underline{A}$ and $\underline{B}$ have their usual significance). This should permit use of the on-line Riccatti method of Banks[3] in which the optimal feedback coefficient matrix is continuously updated (from $\underline{A}$ and $\underline{B}$ matrices that are themselves recalculated continuously from state measurements via the known analytic model). It is intended to evaluate the adaptive control emerging from this potentially powerful approach, using the linear-control predictions (here derived) as a yardstick.

Table 2: Summary of Key Formulae

Tubular Columns

$$S = \frac{\varepsilon\{\varepsilon + 2(\alpha+1)L\}}{(\alpha+1)(2\varepsilon L + \alpha + 1)}$$

$$L = \frac{S(\alpha+1)^2 - (\alpha-1)^2}{2(1-S)(\alpha-1)(\alpha+1)} \quad , \qquad (\frac{\alpha-1}{\alpha+1})^2 < S < 1.0$$

$$G = \frac{2\varepsilon}{(\alpha+1)(2\varepsilon L + \alpha + 1)}$$

$$g_1(p) = G[\frac{\varepsilon(\cosh qL - 1)/p - (1+\alpha)(\sinh qL)/q - \varepsilon/2}{(1-h_e\alpha^{-1})(\sinh qL)q/p + (1+h_e\alpha^{-1})\cosh qL}]$$

$$q^2 = p(p+2) \quad , h_e(p) = 1/(1+Tp)$$

$$g_0 = g_1(0) = \frac{2\alpha\varepsilon\{\varepsilon L^2 - (1+\alpha)L - \varepsilon/2\}}{(\alpha+1)(2\varepsilon L + \alpha + 1)^2}$$

$$\lim_{|p|\to 0} g_1(p) = \frac{g_0}{1+T_0 p}$$

$$T_0 = \frac{\varepsilon L + (\alpha+1)L^2}{2\varepsilon L + \alpha + 1} - \frac{\varepsilon L^2}{2\{\varepsilon L^2 - (1+\alpha)L - \varepsilon/2\}}$$

$$\lim_{|p|\to\infty} g_1(p) = \frac{-g_\infty}{(1+T_\infty p)}$$

$$g_\infty = 2G/(2+\alpha), \quad T > 0$$

$$g_\infty = 2G\alpha/(\alpha+1)^2, \quad T = 0$$

$$T_\infty = 2/(2+\alpha), \quad T > 0$$

$$T_\infty = 2/(1+\alpha), \quad T = 0$$

CSTC Columns

$$S = \frac{\varepsilon}{\alpha+1}[\frac{(3\alpha+1)L + \alpha - 1}{(3\alpha-1)L + \alpha + 1}]$$

$$L = \frac{S(\alpha+1)^2 - (\alpha-1)^2}{(3\alpha+1)(\alpha-1) - S(\alpha+1)(3\alpha-1)}$$

$$\frac{S+1+2\sqrt{S^2-S+1}}{3(1-S)} < \alpha < \frac{S+1+2\sqrt{S}}{1-S}$$

$$g_1(p) = \frac{\alpha\varepsilon}{(\alpha+1)}[\frac{\varepsilon L^2 - 4\alpha L - \varepsilon - pL\{\varepsilon + (\alpha+1)L\}}{\{\alpha+1+(3\alpha-1)L\}[\alpha+1+(3\alpha-1)L + 2\alpha(L+1)Lp + \alpha L^2 p^2]}], \text{ T=0}$$

$$g_0 = g_1(0) = \frac{\alpha\varepsilon}{(\alpha+1)}[\frac{\varepsilon L^2 - 4\alpha L - \varepsilon}{\{(3\alpha-1)L + \alpha + 1\}^2}]$$

$$\lim_{|p|\to 0} g_1(p) = \frac{g_0}{1+T_0 p}$$

$$T_0 = \frac{2\alpha L(L+1)+T(L-1)}{(3\alpha-1)L+\alpha+1} + \frac{L\{\varepsilon+(\alpha+1)L\}}{\varepsilon L^2 - 4\alpha L - \varepsilon}$$

$$\lim_{|p|\to\infty} g\ (p) = \frac{-g_\infty}{1+T_\infty p}$$

$$g_\infty = \frac{\varepsilon\{\varepsilon+(\alpha+1)L\}^2}{(\alpha+1)\{\alpha+1+(3\alpha-1)L\}\{\varepsilon+(3\alpha+1)L^2\}} \qquad \text{and}$$

$$T_\infty = \frac{L\{L(\alpha+1)+\varepsilon\}}{\{L^2(3\alpha+1)+\varepsilon\}}$$

Equations in Common

$\varepsilon = \alpha - 1$, p = Laplace Variable w. r. t (t/T_n)

$L = Lk/V$, $T = H'/VT_n$, $T_n = H/k$

$$g_1(p) = \frac{\delta}{u} = \frac{(y-x')V}{(\upsilon+l)}$$

$$g_A(p) = \frac{g_0(1-T_1 p)}{1+(T_2+T_3)p+T_2T_3p^2}$$

$$T_2 + T_3 = \frac{g_0(T_0 - T_\infty)}{(g_0+g_\infty)}$$

$$T_1 = \frac{g_0T_\infty + g_\infty T_0}{(g_0+g_\infty)}$$

$$T_2T_3 = \frac{g_0T_\infty}{g_\infty}\left[\frac{g_0T_\infty + g_\infty T_0}{g_0+g_\infty}\right]$$

$$K_c g_0 = \frac{g_0(T_0-T_\infty)}{g_0T_\infty + g_\infty T_0}$$

$$E_c = \frac{1}{1+K_c g_0} = \frac{g_0T_\infty + g_\infty T_0}{(g_\infty+g_0)T_0}$$

References

(1) Edwards J. B. : Modelling of chemical process plant, Chap. 2 of Modelling of Dynamical Systems, Ed. H. Nicholson, IEE Control Eng. Series 12, Peregrinus, 1980 pp 25-61

(2) Tabrizi M.N and Edwards, J. B. : Mathl. Comput. Mod., Vol. 16, No. 5, 1992 pp131-146

(3) Banks S. P.and Mhana, K. J: Optimal control and stabilization for nonlinear systems, IMA Journal of Mathematical Control & Information (1992) 9, 179-196.

(4) Edwards J. B and Mohd-Noor S. B : Use of the Riccatti Equation on-line for adaptively controlling a CSTR chemical reactor, University of Sheffield, ACSE Research Report No.576,May 1995.

Appendix 1

Cost Weighting Factor Estimation

The cost to be minimised is

$$C = \int_0^\infty [(S_r - S)^2 + \lambda(\frac{\alpha V_s}{V} - 1)^2]d\tau$$

where V is the steady-state rectifier vapour flow rate used to determine normalised length (L=kL'/V) and which yields the designed reference separation S_r according to eq^n. (39) in steady-state. Choice if this cost function ensures that C will not continue to integrate once the desired steady state S=Sr is achieved. The virtue of ensuring consistent input and output references (Sr and V/α in this application) is demonstrated in ACSE Research Report 576[4]. Choosing inconsistent values causes $\partial C/\partial\tau$ to be nonzero in steady-state even under optimal control leading to complications with the Riccatti solution.

The choice of λ will be clearly affected by the relative significance of the integrand error terms Sr-S and V_s-αV. If there are to be of roughly equal significance then clearly

$$\lambda = [\frac{(S_r - S)V}{(\alpha V_s - V)}]^2$$

Now from our linear analysis of Section 3. 1

$$g_1(0) = \delta / u = \delta V / 2\upsilon$$

where δ and υ are deviations in separation and vapour rate from their steady-state conditions. Hence, as a coarse approximation, setting

$$\delta = S_r - S$$

and $\upsilon = V/\alpha - V_s$

then $g_1(0) \cong \frac{(S_r - S)V}{(V/a - V_s)2} = \frac{(S_r - S)V}{(V - \alpha V_s)} \times \frac{\alpha}{2}$

Hence for roughly equal cost weighting of separation and flow errors

$$\lambda \cong (2g_1(0)/\alpha)^2$$

g1(0) can be obtained from eq^n. (84), given values of L', k, V and α. The linear analysis is therefore useful for generating initial estimates of λ in the optimal control design. For control over a wide range of state space, experimental tuning of the value of λ will be necessary of course.

Acknowledgement

The authors wish to acknowledge Professor P. J. Flemming, Head of ACSE for the use of Department facilities in producing this report and in undertaking this research. The work was partially supported also by EPSRC grant No. GR/J75241 for which the authors wish to express gratitude.

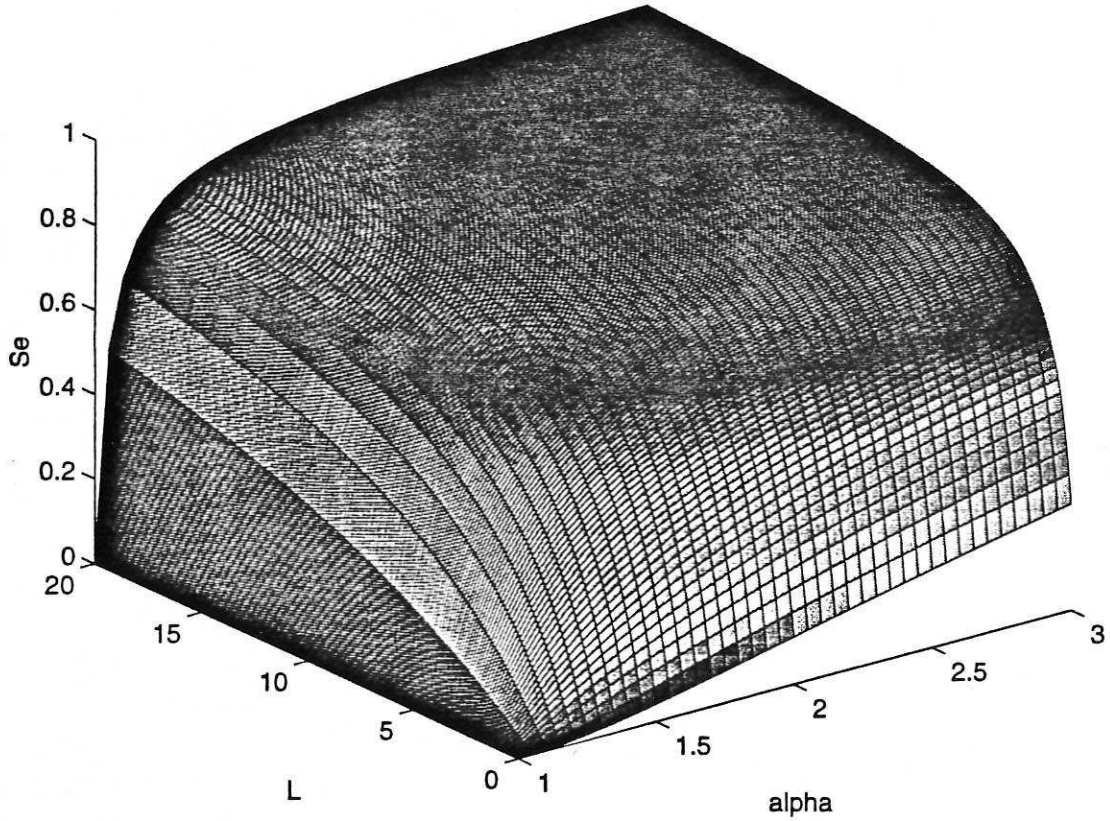

Figure 1. Variation of separation in tubular column with L and α

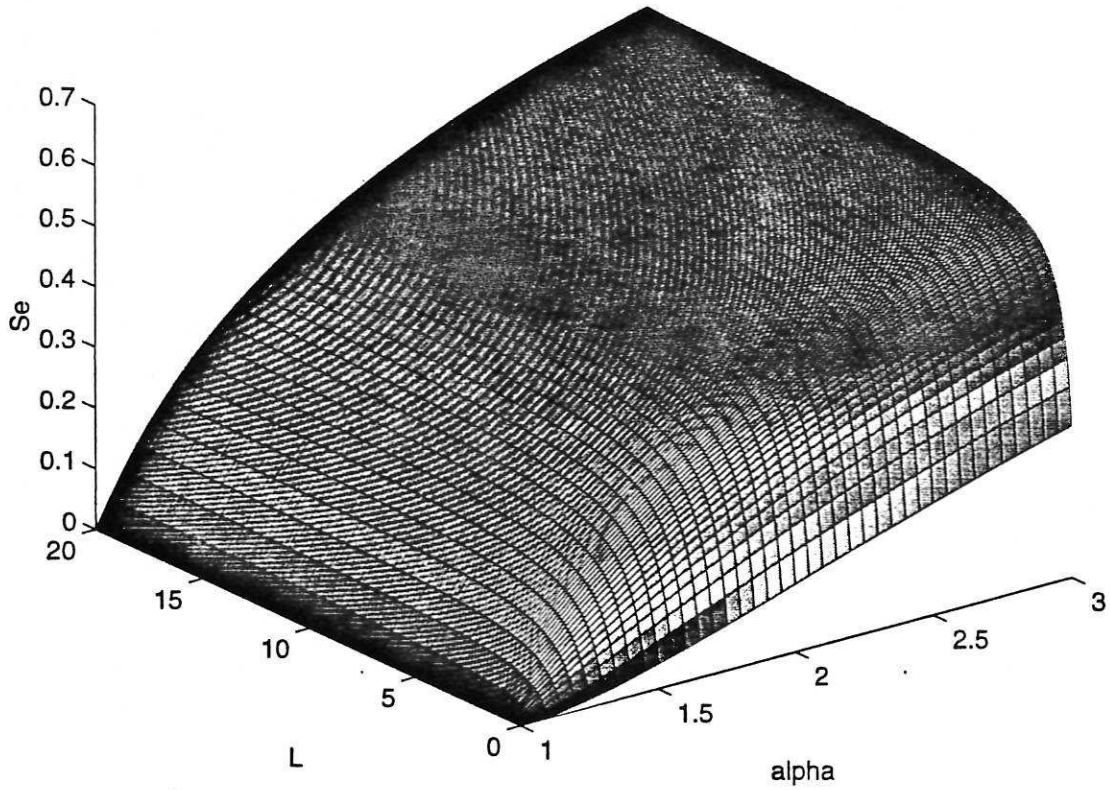

Figure 2. Variation of separation in CSTC column with L and α

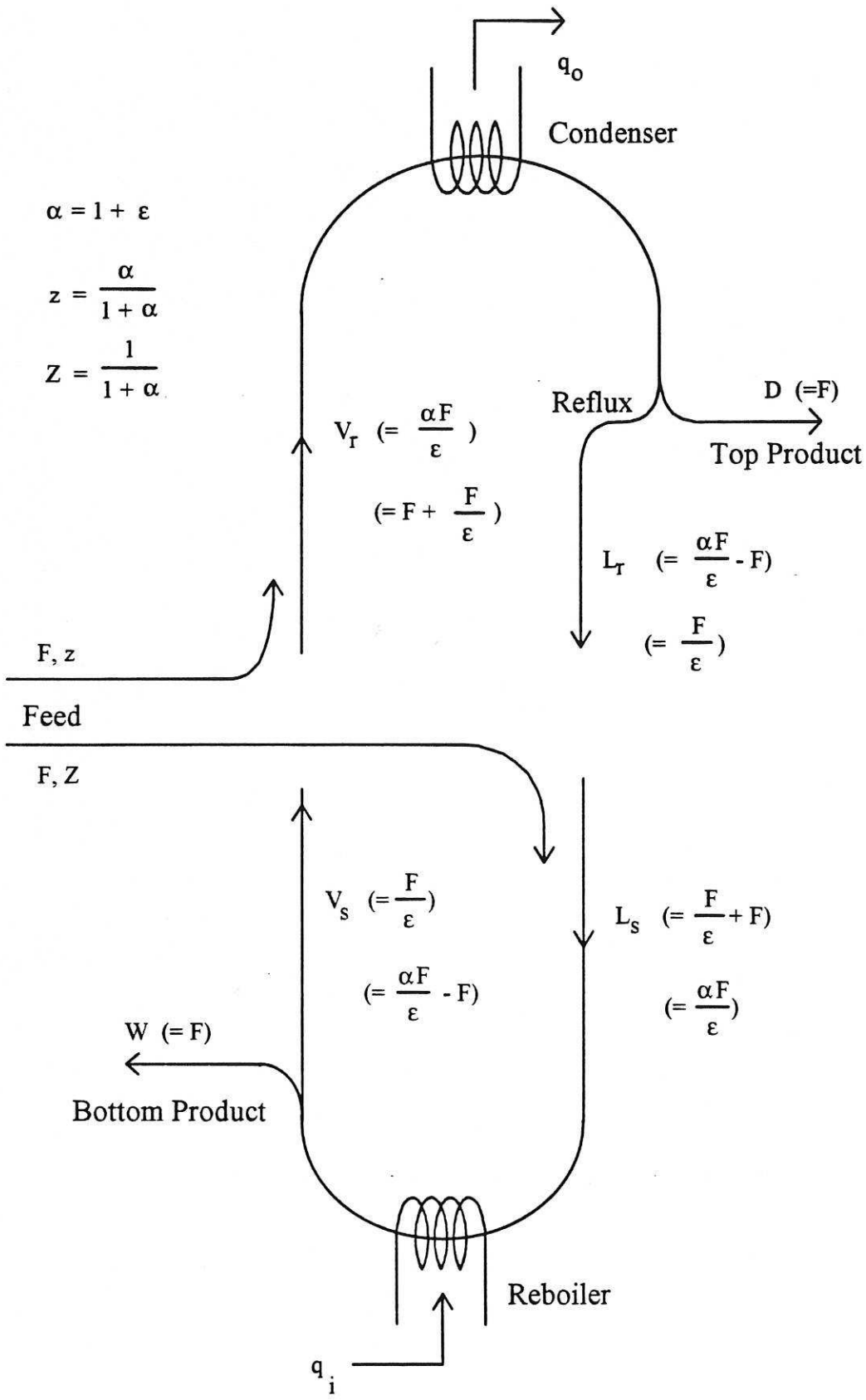

Figure 3: Steady-state operating conditions : Quiescent Flow Summary Diagram

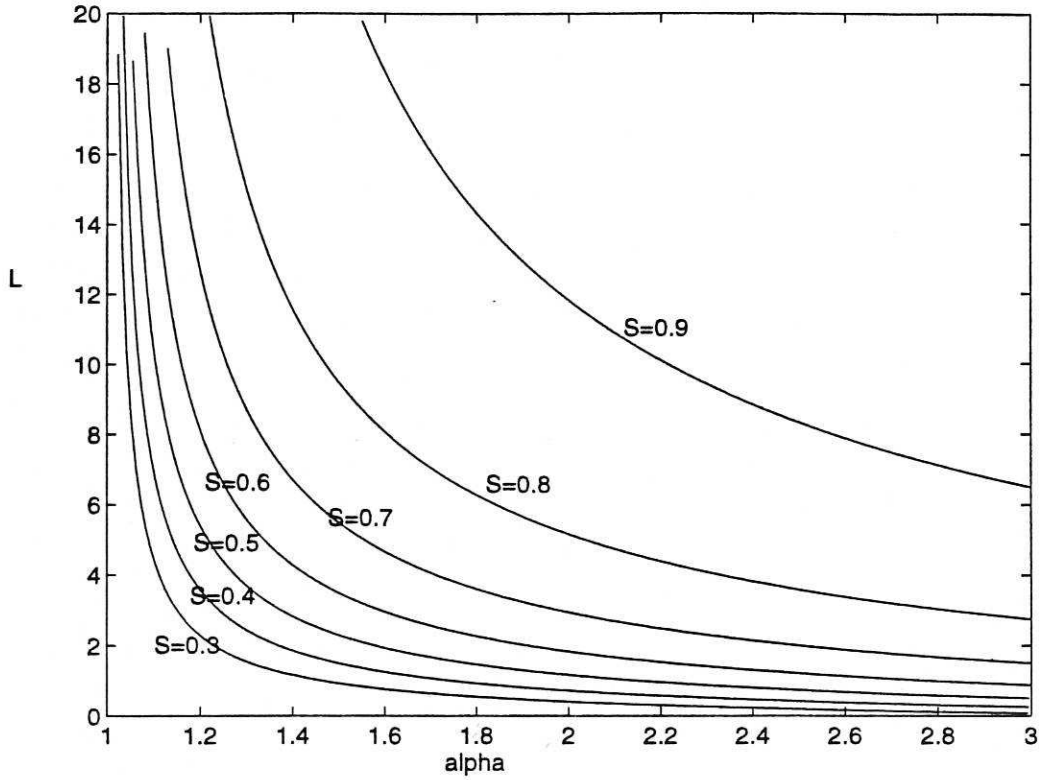

Figure 4. Constant separation loci of L versus α for tubular column.

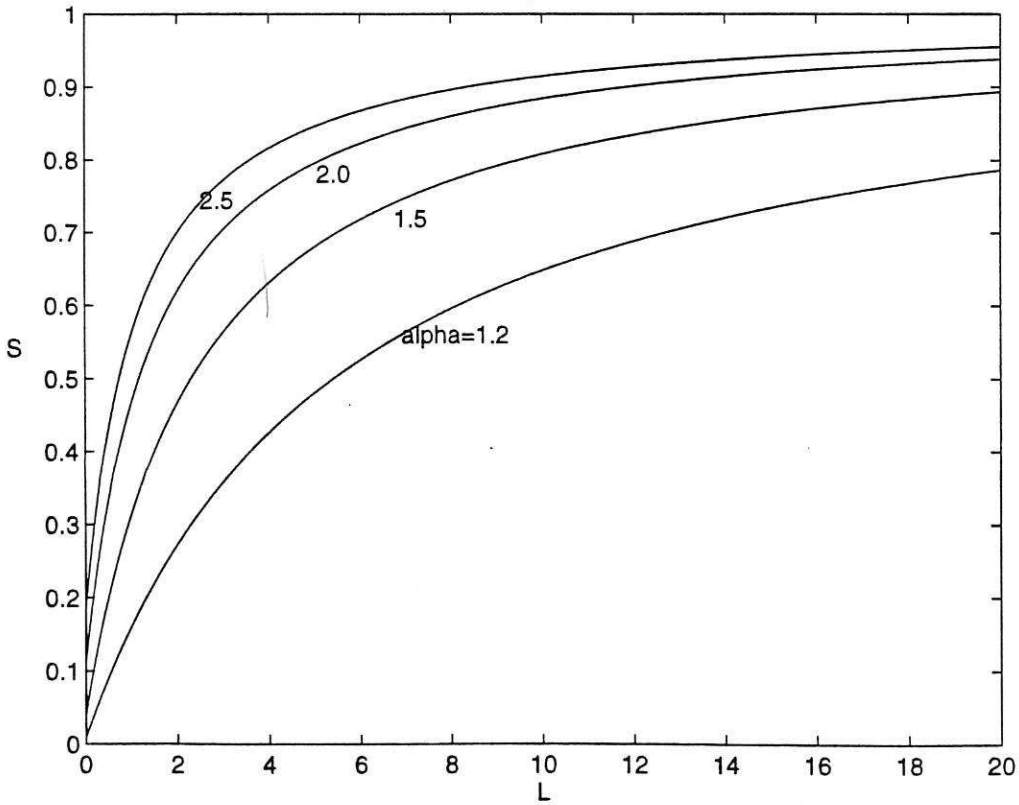

Figure 5. Variation of separation with normalised column length for selected α-values : Tubular column

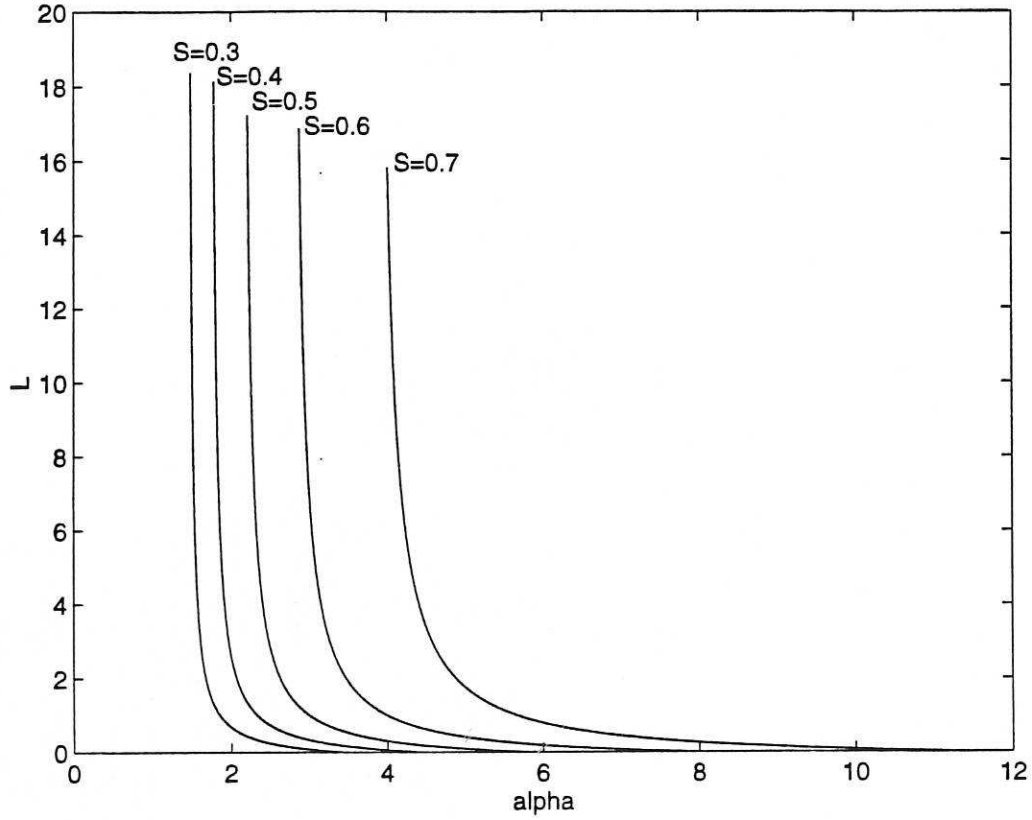

Figure 6. Constant separation loci of L versus α for CSTC Column

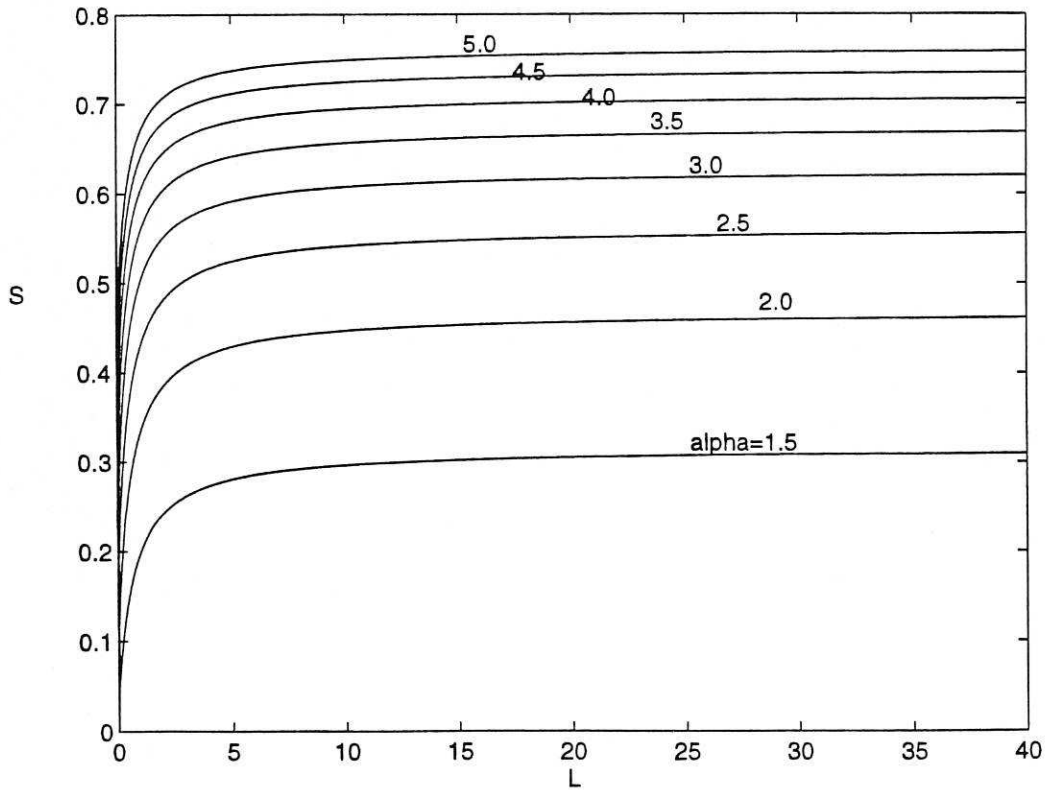

Figure 7. Variation of separation with normalised column length for selected α-values CSTC Column

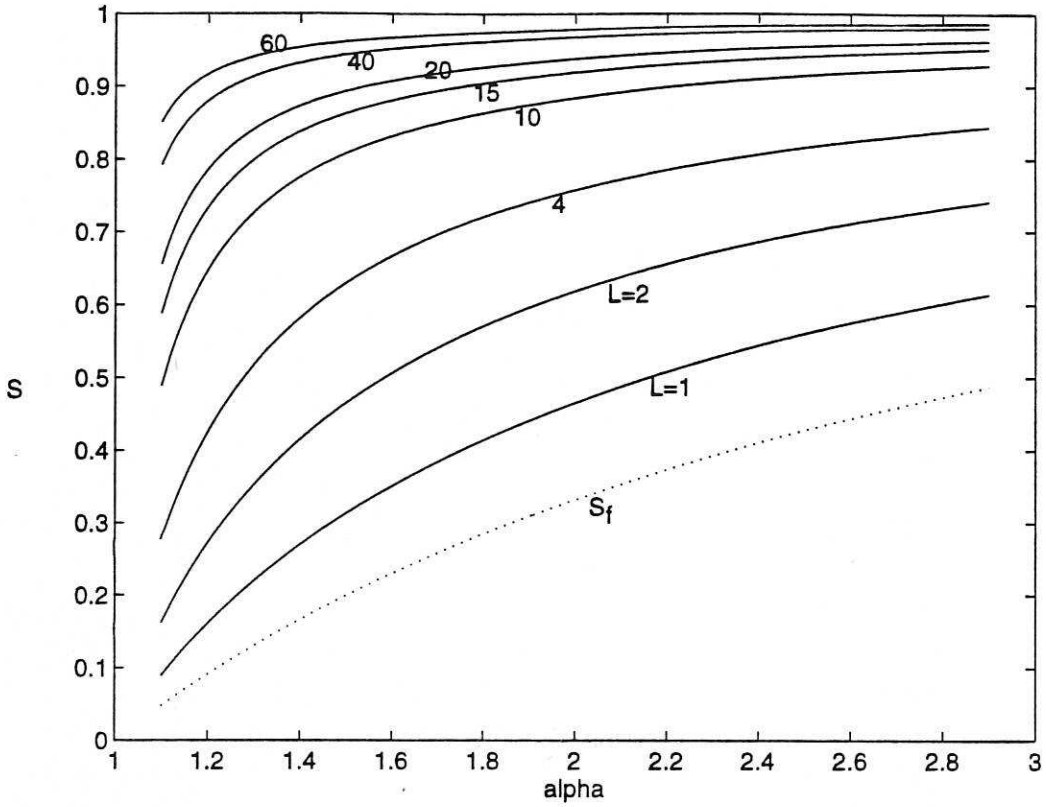

Figure 8. Separation versus α for selected values of L : Tubular Column

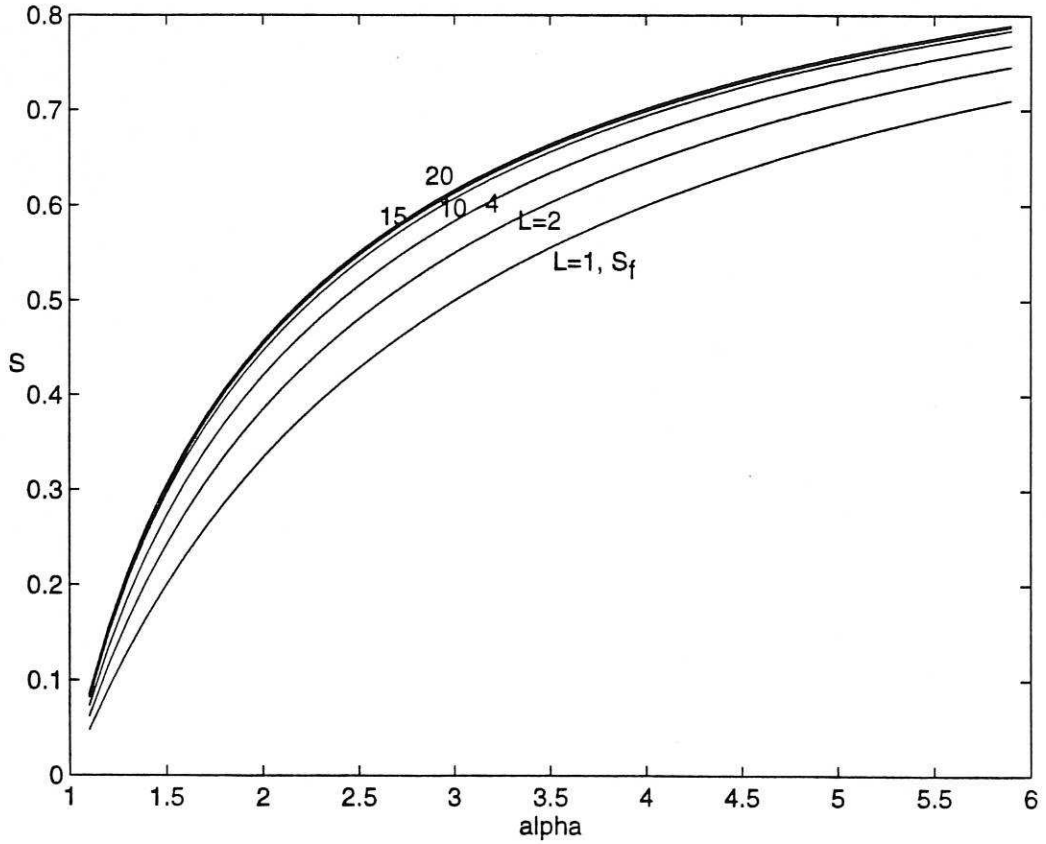

Figure 9. Separation versus α for selected values of L : CSTC Column

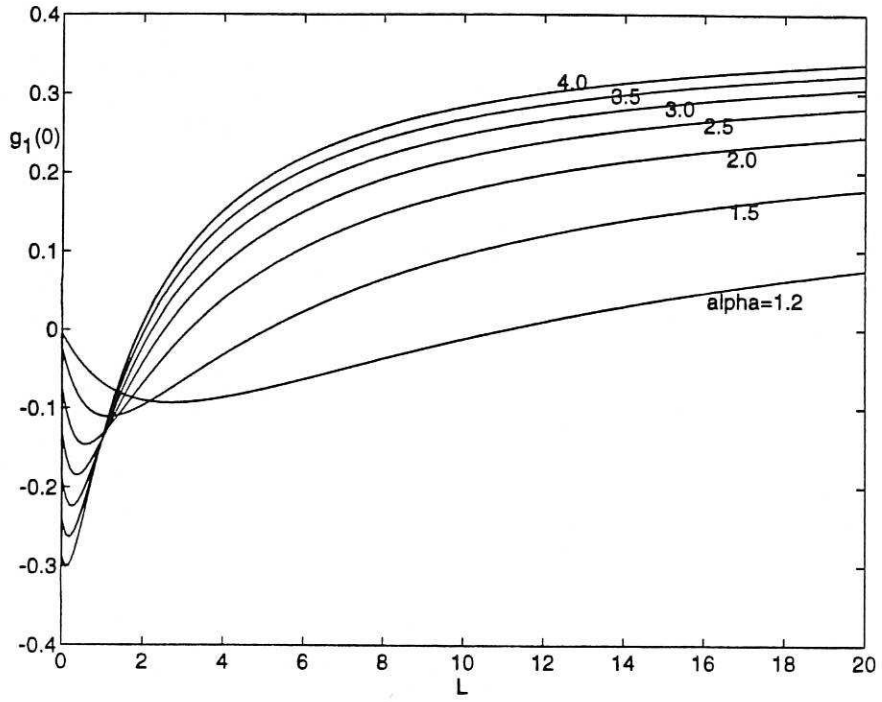

Figure 10. Variation of gain with L for selected α : Tubular Column

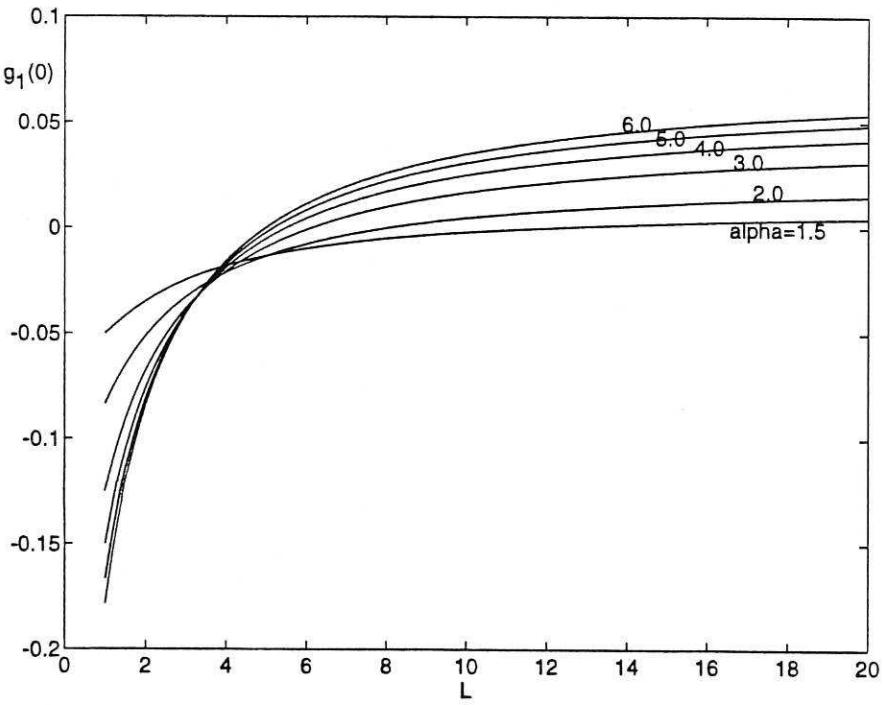

Figure 11. Variation of gain with L for selected α : CSTC Column

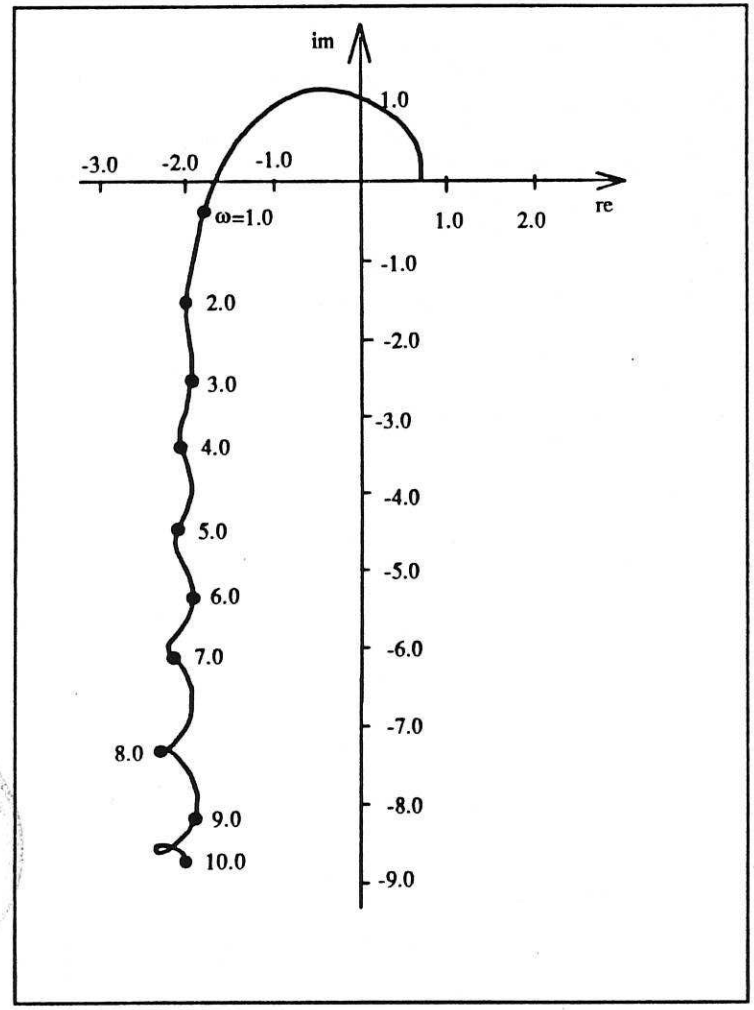

Figure 12. Inverse Nyquist locus of $g_1^{-1}(j\omega)$ for tubular column: $\alpha=2$, L=5, T=20

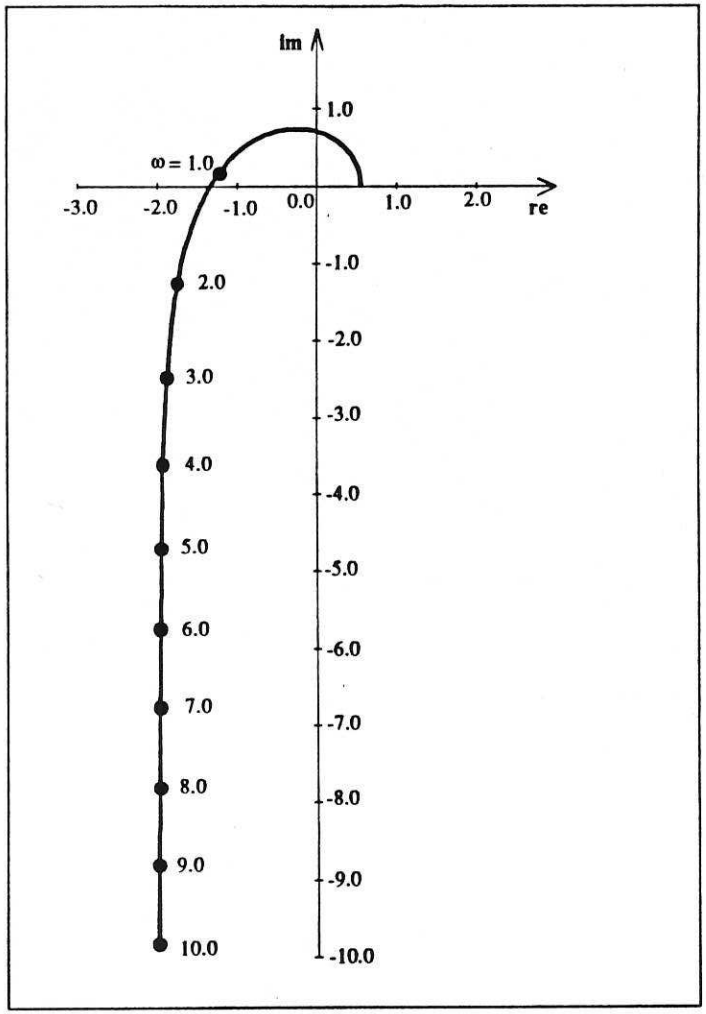

Figure 13. Inverse Nyquist locus of $g_A^{-1}(j\omega)$ approximation for tubular column: $\alpha=2$, L=5, T=20